Accumulation-driven synchronization in phase oscillators with endogenous coupling

Ori Manzur[a,*]

[a] reBORN Research Initiative, Israel

ARTICLE INFO

Keywords:
Phase oscillators
Endogenous coupling
Adaptive synchronization
Fast–slow dynamics
Threshold dynamics
Phase locking

ABSTRACT

In fixed-coupling phase oscillator systems, frozen phase-locked states exist only when coupling exceeds the detuning threshold; below this threshold, trajectories drift. This raises the question of how synchronization-like capture can arise from an initially subthreshold state when coupling evolves endogenously.

We introduce a class of phase oscillator systems in which effective coupling is generated through a compatibility–integration cascade. Internal variables accumulate compatibility-window exposure along the trajectory, rather than coupling being prescribed directly by instantaneous phase differences.

Under the stated structural assumptions, we show that on compact uniformly subthreshold intervals, detuned trajectories traverse the compatibility window whenever the lifted phase completes rotations. These traversals generate compatibility-window exposure, giving a guaranteed positive contribution to monotone growth of the integration variables and monotone amplification of effective coupling. Sufficient accumulated exposure implies finite-time crossing of the compatibility-window threshold.

After this threshold is crossed, the compatibility window becomes forward-invariant. Trajectories entering the window after threshold crossing are captured, and on finite post-capture intervals satisfy a tracking estimate relative to the moving frozen equilibrium branch, consisting of an exponentially decaying entry-error term plus an $O(\epsilon)$ forcing term.

This establishes a conditional synchronization-like capture mechanism in which drift/traversal contributes to threshold crossing through exposure-driven accumulation and amplification. Under genuine hidden-state dependence, the mechanism cannot be reproduced by universal phase-only adaptive coupling laws of the form $\dot{K} = f(\phi)$. Numerical simulations illustrate one admissible trajectory exhibiting the predicted conditional sequence.

1. Introduction

1.1. Motivation: synchronization and evolving interactions

Synchronization in coupled oscillator systems is a central phenomenon in nonlinear dynamics, where collective behavior emerges from interactions between individual units. In phase oscillator models, synchronization is governed by the interplay between intrinsic frequency differences and coupling strength.

In the classical Kuramoto framework, coupling is fixed and prescribed. In the two-oscillator phase-difference reduction, frozen phase-locked equilibria exist only when the coupling exceeds the detuning threshold; otherwise, the system remains in a drift regime. Thus, in fixed-coupling models, the existence of frozen locked states is determined by instantaneous parameters.

In many systems, however, interaction strengths are not fixed but evolve in response to the system state. This has led to the study of adaptive and co-evolving oscillator models, in which coupling itself becomes a dynamical variable.

Literature positioning. The relationship between detuning, coupling strength, and phase locking is classical in phase oscillator theory, including the Adler equation and Kuramoto-type reductions [2, 9, 12, 1, 11]. Adaptive and co-evolving oscillator models extend this setting by allowing coupling strengths, weights, or interaction parameters to evolve dynamically [3, 4, 8, 6]. The present work is positioned within this adaptive-coupling tradition, but focuses on a specific mechanism in which compatibility-window exposure is accumulated through hidden integration variables before affecting the effective coupling.

*Corresponding author.
manzurori4@gmail.com (O. Manzur)

1.2. Limitations of direct adaptive coupling models

In many phase-only adaptive formulations, coupling evolves according to rules of the form

$$\dot{K}_{ij} = f(\phi_i - \phi_j), \tag{1}$$

so that interaction strength is updated directly from instantaneous phase differences, as in adaptive and co-evolving phase-oscillator formulations [3, 4, 6].

Such phase-only adaptive laws can exhibit rich behavior, but share a common structural feature: at the level of the update rule, coupling evolution is determined by the current phase configuration and does not incorporate separate hidden integration variables that encode compatibility-exposure history. As a result:

- coupling updates are phase-local at the level of the update rule;
- separate compatibility-exposure accumulation is not explicitly represented;
- synchronization behavior remains tied to the chosen phase-coupling feedback rule.

In particular, such formulations do not isolate the mechanism studied here, in which repeated compatibility-window exposure is accumulated through additional integration variables and may drive compatibility-threshold crossing.

1.3. Compatibility–integration formulation

We consider an alternative formulation in which coupling is not prescribed as a function of phase difference, but is generated through a compatibility–integration cascade.

In this framework:

- a scalar incompatibility functional quantifies instantaneous misalignment;
- internal variables accumulate compatibility exposure over time;
- effective coupling is generated as a function of these accumulated variables.

This structure separates fast phase dynamics from slow integration-mediated coupling evolution and introduces memory into the phase-projected dynamics. As a result, the coupling at a given time reflects the accumulated history of compatibility exposure along the trajectory rather than the instantaneous phase value alone.

1.4. Contributions and main results

The main contribution of this work is the identification and rigorous analysis of a conditional accumulation-driven mechanism for synchronization-like capture. The present model isolates a phase-oscillator mechanism inspired by a broader unpublished framework on compatibility-modulated stability thresholds [10]. Under the stated structural assumptions, we show that:

- on compact uniformly subthreshold intervals, drift dynamics produce traversal of the compatibility window whenever the lifted phase completes rotations;
- these traversals produce compatibility-window exposure, which gives a guaranteed positive contribution to the monotone growth of the integration variables;
- the resulting accumulation drives monotone amplification of the effective coupling;
- the compatibility-window threshold is crossed when sufficient compatibility-window exposure is accumulated;
- after threshold crossing, the compatibility window becomes forward-invariant, and trajectories are captured upon post-threshold entry;
- captured trajectories satisfy finite-interval tracking of the moving frozen equilibrium branch, with full $O(\varepsilon)$ tracking only when the entry error is $O(\varepsilon)$.

Together, these results establish a conditional mechanism in which synchronization-like capture may emerge from an initially subthreshold state through exposure-driven accumulation, compatibility-window threshold crossing, and post-threshold entry, rather than through instantaneous alignment or direct phase-only coupling updates.

1.5. Organization of the paper

Section 2 introduces the model and states the structural assumptions. Section 3 analyzes the reduced dynamics and the behavior of the incompatibility functional. Section 4 characterizes the frozen-system threshold structure, distinguishing between equilibrium-existence and compatibility-window thresholds. Section 5 establishes the conditional exposure-driven threshold crossing, capture, and finite-interval tracking mechanism. Section 6 interprets the resulting conditional dynamics. Section 7 provides a numerical illustration of one admissible trajectory exhibiting the conditional mechanism. Section 8 positions the results relative to existing approaches and discusses extensions. Section 9 concludes.

2. Model formulation

2.1. Phase oscillator system with endogenous coupling

We consider a system of two coupled phase oscillators whose interaction strength is generated through internal variables, within the standard phase-oscillator modeling framework [9, 11, 1, 7]. Let $\theta_1(t), \theta_2(t) \in \mathbb{S}^1$ denote the phases, and $\omega_1, \omega_2 \in \mathbb{R}$ their natural frequencies. The dynamics are

$$\begin{aligned} \dot{\theta}_1 &= \omega_1 + K_{\text{tot}}(\Gamma_1, \Gamma_2)\sin(\theta_2 - \theta_1), \\ \dot{\theta}_2 &= \omega_2 + K_{\text{tot}}(\Gamma_1, \Gamma_2)\sin(\theta_1 - \theta_2), \end{aligned} \tag{2}$$

where $\Gamma_i(t) \geq 0$ are internal variables and $K_{\text{tot}}(\Gamma_1, \Gamma_2)$ is the effective coupling.

Phase difference reduction. Define

$$\phi = \theta_2 - \theta_1, \qquad \Delta\omega = \omega_2 - \omega_1.$$

A direct subtraction yields

$$\dot{\phi} = \Delta\omega - 2K_{\text{tot}}(\Gamma_1, \Gamma_2)\sin\phi.$$

Following the normalization introduced in Section 3.1, we absorb the factor of 2 into the definition of K_{tot}, and write

$$\dot{\phi} = \Delta\omega - K_{\text{tot}}(\Gamma_1, \Gamma_2)\sin\phi. \tag{3}$$

This scalar equation, coupled with the evolution of Γ_i, is the primary object of analysis.

Fast–slow structure. On bounded trajectory sets where the integration rates H_i remain bounded, the system exhibits a fast–slow decomposition:

$$\dot{\phi} = O(1), \qquad \dot{\Gamma}_i = O(\varepsilon).$$

Thus, for sufficiently small $0 < \varepsilon \leq \varepsilon_0$, the variables Γ_i evolve on a slower timescale than the phase dynamics.

Coupling dependence. The effective coupling $K_{\text{tot}}(\Gamma_1, \Gamma_2)$ depends on the internal variables Γ_i. Its value at time t is therefore determined by the accumulated evolution of these variables rather than by the instantaneous phase value alone.

2.2. Incompatibility functional

We introduce a scalar functional measuring misalignment between the oscillators.

Definition. Let $\phi \in \mathbb{S}^1$. Define

$$F(\phi) = 1 - \cos\phi. \tag{4}$$

Basic properties. The function $F : \mathbb{S}^1 \to [0, 2]$ is smooth and satisfies

$$F(\phi) \geq 0, \qquad F(\phi) = 0 \quad \Longleftrightarrow \quad \phi = 0 \pmod{2\pi},$$

and

$$\max F = 2 \quad \text{at} \quad \phi = \pi \pmod{2\pi}.$$

Local behavior. On the representative interval $[-\pi, \pi]$, F is even and strictly increasing on $[0, \pi]$. Moreover,

$$F(\phi) = \frac{1}{2}\phi^2 + O(\phi^4) \qquad \text{as } \phi \to 0.$$

Role in the model. The functional $F(\phi)$ serves as the input to the integration dynamics, providing a scalar measure of instantaneous misalignment that drives the evolution of the internal variables Γ_i. In particular, intervals of low incompatibility, characterized by small $|\phi|$, correspond to small values of F and play a distinguished role in the accumulation mechanism developed in Section 5.

2.3. Compatibility–integration cascade

We define the evolution of the internal variables and the resulting generation of effective coupling.

Integration dynamics. Each oscillator is associated with an internal variable $\Gamma_i(t) \geq 0$, evolving as

$$\dot{\Gamma}_i = \varepsilon H_i(F(\phi), \Gamma_i), \qquad i = 1, 2, \tag{5}$$

where $F(\phi)$ is defined in Section 2.2, H_i is locally Lipschitz in its arguments, and $0 < \varepsilon \leq \varepsilon_0$ sets the timescale separation. We assume $\Gamma_i(0) \geq 0$.

Compatibility-driven growth. The functions H_i depend on $F(\phi)$ such that intervals of low incompatibility, corresponding to small $F(\phi)$, contribute positively to the growth of Γ_i. In particular, under the assumptions specified in Section 2.4, there exists a compatibility window in which the growth rate is uniformly bounded below.

Effective coupling. The effective coupling is defined by

$$K_{\text{tot}} = K_{\text{tot}}(\Gamma_1, \Gamma_2),$$

where K_{tot} is continuous and non-decreasing in each argument. The additional regularity required for post-capture tracking estimates is stated separately in Assumption (A6).

Cascade structure. The interaction is given by

$$\phi \longmapsto F(\phi) \longmapsto \Gamma_i \longmapsto K_{\text{tot}}.$$

Remark 1. *The dependence of K_{tot} on Γ_i implies that the coupling is determined by the accumulated evolution of the system and therefore depends on the trajectory history rather than on the instantaneous phase value alone. This introduces a form of memory into the phase-projected dynamics, which underlies the conditional accumulation-driven mechanism developed in Section 5.*

2.4. Structural assumptions

We state the assumptions on H_i and K_{tot} defining the admissible class of systems.

(A1) Non-negativity of integration dynamics. For all $F \in [0, 2]$ and all $\Gamma_i \geq 0$,

$$H_i(F, \Gamma_i) \geq 0, \qquad i = 1, 2. \tag{6}$$

(A2) Positive growth inside the compatibility window. There exist $\bar{\phi} \in (0, \pi/2)$ and constants $h_i > 0$ such that

$$H_i(F(\phi), \Gamma_i) \geq h_i \tag{7}$$

for all

$$\phi \in U_{\bar{\phi}} := (-\bar{\phi}, \bar{\phi}) \tag{8}$$

and all $\Gamma_i \geq 0$. Thus, within the compatibility window $U_{\bar{\phi}}$, the integration variables grow at a uniformly positive rate.

(A3) Non-negative monotone coupling amplification. The map

$$K_{\text{tot}} : \mathbb{R}_+^2 \to [0, \infty)$$

is continuous and non-decreasing in each argument.

(A4) Timescale separation. There exists a fixed $\varepsilon_0 > 0$ such that

$$0 < \varepsilon \le \varepsilon_0.$$

All $O(\varepsilon)$ estimates are understood on finite intervals of fixed length, with constants depending on the interval length and the bounded trajectory set under consideration, but not on ε. In the post-capture tracking result, these intervals may be shifted intervals

$$[t_*(\varepsilon), t_*(\varepsilon) + L],$$

with $L < \infty$ fixed independently of ε, provided the corresponding slow variables remain in an ε-independent compact subset of $\mathbb{R}^2_+$.

(A5) Compatibility-threshold reachability. There exists

$$\Gamma^* = (\Gamma_1^*, \Gamma_2^*) \in \mathbb{R}^2_+$$

such that

$$|\Delta\omega| < K_{\mathrm{tot}}(\Gamma^*) \sin \bar{\phi}. \tag{9}$$

This condition is a reachability condition on the coupling function. It is not a trajectory-level threshold-crossing assumption. It only states that the coupling architecture can place the system above the compatibility-window threshold for sufficiently large integration states.

(A6) Coupling regularity for tracking estimates. The coupling function K_{tot} extends to a C^1 function on an open neighborhood of every compact subset of $\mathbb{R}^2_+$, and its partial derivatives are locally bounded. Equivalently, for every compact set $B \subset \mathbb{R}^2_+$, there exists $C_B > 0$ such that

$$\left| \frac{\partial K_{\mathrm{tot}}}{\partial \Gamma_i}(\Gamma) \right| \le C_B, \qquad i = 1, 2, \qquad \Gamma \in B. \tag{10}$$

Pairwise coupling structure. The effective coupling depends only on the integration variables (Γ_1, Γ_2) associated with the interacting pair and introduces no additional interaction channels. This structural restriction is part of the model formulation, but it is not used as a numbered assumption in the theorem statement.

Remark 2. *These assumptions ensure non-negative accumulation of the integration variables, monotone amplification of coupling, reachability of the compatibility-window threshold at the level of the coupling function, and sufficient regularity for finite-interval post-capture tracking estimates.*

Trajectory-level threshold crossing is not assumed unconditionally. It is addressed in Section 5 through exposure-based sufficient conditions.

All dynamical conclusions are understood on the maximal forward interval of existence of the corresponding solution. If one additionally assumes global forward existence, for example through suitable growth bounds on the integration dynamics and coupling function, then the same conclusions hold globally in forward time.

3. Reduced dynamics and basic properties

3.1. Phase difference reduction

We reduce the system defined in Section 2 to a scalar equation governing the phase difference.

Derivation. Let $\theta_1(t), \theta_2(t) \in \mathbb{S}^1$ satisfy

$$\dot{\theta}_1 = \omega_1 + K_{\mathrm{tot}}(\Gamma_1, \Gamma_2) \sin(\theta_2 - \theta_1),$$

$$\dot{\theta}_2 = \omega_2 + K_{\mathrm{tot}}(\Gamma_1, \Gamma_2) \sin(\theta_1 - \theta_2).$$

Define

$$\phi = \theta_2 - \theta_1.$$

Then

$$\dot{\phi} = \dot{\theta}_2 - \dot{\theta}_1 = (\omega_2 - \omega_1) - 2K_{\mathrm{tot}}(\Gamma_1, \Gamma_2) \sin \phi.$$

Normalization. For notational convenience, we redefine

$$K_{\mathrm{tot}} \leftarrow 2K_{\mathrm{tot}},$$

so that the reduced equation becomes

$$\dot{\phi} = \Delta\omega - K_{\mathrm{tot}}(\Gamma_1, \Gamma_2)\sin\phi,$$

where

$$\Delta\omega = \omega_2 - \omega_1.$$

This normalization is used throughout the remainder of the paper.

Result. The dynamics reduce to a scalar phase equation coupled to the slow evolution of Γ_i. This equation forms the basis for the analysis of frozen drift, threshold structure, and the conditional accumulation-driven capture mechanism developed in Sections 4–5.

3.2. Evolution of the incompatibility functional

We compute the evolution of the incompatibility functional $F(\phi)$ along trajectories of the reduced phase dynamics.

Time derivative. Recall

$$F(\phi) = 1 - \cos\phi.$$

Along trajectories,

$$\frac{d}{dt}F(\phi(t)) = \sin\phi(t)\dot{\phi}(t).$$

Using

$$\dot{\phi} = \Delta\omega - K_{\mathrm{tot}}(\Gamma_1, \Gamma_2)\sin\phi,$$

we obtain, along trajectories,

$$\frac{d}{dt}F(\phi(t)) = \Delta\omega\sin\phi(t) - K_{\mathrm{tot}}(\Gamma_1, \Gamma_2)\sin^2\phi(t). \tag{11}$$

Structure of the dynamics. The evolution of $F(\phi)$ consists of two contributions:

- a term $\Delta\omega\sin\phi$, which may change sign;
- a term $-K_{\mathrm{tot}}(\Gamma_1, \Gamma_2)\sin^2\phi \le 0$.

Thus, the sign of $\frac{d}{dt}F(\phi(t))$ is not fixed in general.

Consequence. In the presence of detuning ($\Delta\omega \neq 0$), the incompatibility functional is not monotone along trajectories. This non-monotonicity contrasts with the resonant case considered in Section 3.3 and motivates the accumulation mechanism developed later, where integration occurs over repeated intervals of low incompatibility rather than through monotone decay.

3.3. Resonant case: monotone incompatibility under positive coupling

We consider the case of zero detuning.

Resonant dynamics. Assume

$$\Delta\omega = 0.$$

Then

$$\dot{\phi} = -K_{\mathrm{tot}}(\Gamma_1, \Gamma_2)\sin\phi.$$

The statements below concern the phase dynamics when $K_{\mathrm{tot}}(\Gamma_1, \Gamma_2)$ is treated as fixed, or along trajectories for which the displayed expression is evaluated instantaneously.

Evolution of incompatibility. From Section 3.2,

$$\frac{d}{dt}F(\phi(t)) = -K_{\text{tot}}(\Gamma_1, \Gamma_2)\sin^2\phi(t) \le 0.$$

If $K_{\text{tot}}(\Gamma_1, \Gamma_2) > 0$, equality holds if and only if

$$\phi \in \{0, \pi\} \pmod{2\pi}.$$

Consequence. Thus, for positive fixed coupling, $F(\phi)$ is non-increasing along phase trajectories and strictly decreasing away from the resonant equilibria.

Equilibria. The equilibria are

$$\phi = 0 \quad \text{and} \quad \phi = \pi \pmod{2\pi}.$$

The in-phase state $\phi = 0$ is stable, while $\phi = \pi$ is unstable.

Result. For the frozen resonant phase dynamics with positive coupling, the in-phase state

$$\phi = 0 \pmod{2\pi}$$

is attracting, while

$$\phi = \pi \pmod{2\pi}$$

is unstable.

3.4. Detuned case: drift and equilibrium-existence threshold

We consider the case $\Delta\omega \neq 0$.

Phase dynamics. The reduced equation is

$$\dot{\phi} = \Delta\omega - K_{\text{tot}}(\Gamma_1, \Gamma_2)\sin\phi.$$

Non-monotonic incompatibility. From Section 3.2,

$$\frac{d}{dt}F(\phi(t)) = \Delta\omega\sin\phi(t) - K_{\text{tot}}(\Gamma_1, \Gamma_2)\sin^2\phi(t),$$

so $\frac{d}{dt}F(\phi(t))$ does not have a fixed sign in general.

Drift regime. For fixed (Γ_1, Γ_2), if

$$K_{\text{tot}}(\Gamma_1, \Gamma_2) < |\Delta\omega|,$$

then $\dot{\phi}$ does not vanish and does not change sign. Hence the lifted phase evolves monotonically, and the projected phase performs continuous rotations on $\mathbb{S}^1$.

Equilibrium regime: frozen dynamics. If

$$K_{\text{tot}}(\Gamma_1, \Gamma_2) > |\Delta\omega|,$$

then there exist equilibria satisfying

$$\Delta\omega = K_{\text{tot}}(\Gamma_1, \Gamma_2)\sin\phi.$$

Equilibrium threshold. The transition between drift and the existence of equilibria in the frozen system occurs at

$$K_{\text{tot}}(\Gamma_1, \Gamma_2) = |\Delta\omega|. \tag{12}$$

This condition will be referred to as the equilibrium-existence threshold.

Consequence. In the frozen drift regime, trajectories rotate on $\mathbb{S}^1$ and traverse every open interval during each full rotation. This repeated traversal property provides the foundation for the accumulation mechanism developed in Section 5.

The transition to capture, however, requires the stronger compatibility-window threshold introduced in Section 4, together with the time-dependent exposure and post-threshold entry conditions developed in Section 5.

4. Instantaneous locking and threshold structure

4.1. Local locking condition

We analyze the phase dynamics with fixed coupling, i.e., with Γ_i held constant. In this setting, $K_{\text{tot}}(\Gamma_1, \Gamma_2)$ is treated as a fixed parameter, corresponding to the frozen-coupling limit of the full system.

Frozen dynamics. For fixed (Γ_1, Γ_2),

$$\dot{\phi} = \Delta\omega - K_{\text{tot}}(\Gamma_1, \Gamma_2) \sin \phi.$$

Equilibria. A phase-locked state satisfies

$$\Delta\omega = K_{\text{tot}}(\Gamma_1, \Gamma_2) \sin \phi^*.$$

Such a solution exists if and only if

$$|\Delta\omega| \leq K_{\text{tot}}(\Gamma_1, \Gamma_2).$$

Equilibrium-existence condition. A necessary and sufficient condition for the existence of frozen equilibria is

$$K_{\text{tot}}(\Gamma_1, \Gamma_2) \geq |\Delta\omega|.$$

For

$$K_{\text{tot}}(\Gamma_1, \Gamma_2) > |\Delta\omega|,$$

these equilibria form nondegenerate stable and unstable branches. This condition will be referred to as the equilibrium-existence threshold.

Consequence. If

$$K_{\text{tot}}(\Gamma_1, \Gamma_2) < |\Delta\omega|,$$

the phase velocity does not vanish and the system exhibits drift. If

$$K_{\text{tot}}(\Gamma_1, \Gamma_2) > |\Delta\omega|,$$

nondegenerate equilibrium branches exist. At equality, the frozen system has a degenerate saddle-node equilibrium.

4.2. Existence and stability of frozen locked branches

We analyze the equilibria of the frozen phase dynamics and their stability.

Equilibria. For fixed (Γ_1, Γ_2), equilibria ϕ^* satisfy

$$\Delta\omega = K_{\text{tot}}(\Gamma_1, \Gamma_2) \sin \phi^*.$$

If

$$K_{\text{tot}}(\Gamma_1, \Gamma_2) > |\Delta\omega|,$$

this equation admits two solutions per period, satisfying

$$\sin \phi^* = \frac{\Delta\omega}{K_{\text{tot}}(\Gamma_1, \Gamma_2)}.$$

Stability. The linearization of the vector field is

$$\frac{d}{d\phi}\left(\Delta\omega - K_{\text{tot}}(\Gamma_1, \Gamma_2)\sin\phi\right) = -K_{\text{tot}}(\Gamma_1, \Gamma_2)\cos\phi.$$

An equilibrium ϕ^* is:

- stable if $\cos\phi^* > 0$;
- unstable if $\cos\phi^* < 0$.

Branches. Accordingly:

- the equilibrium with $\phi^* \in (-\pi/2, \pi/2)$ is stable;
- the equilibrium with $\phi^* \in (\pi/2, 3\pi/2) \pmod{2\pi}$ is unstable.

The coexistence of stable and unstable branches helps organize the phase-line structure used in Section 5.

Degenerate case. If

$$K_{\text{tot}}(\Gamma_1, \Gamma_2) = |\Delta\omega|,$$

the equilibria coalesce at $|\phi^*| = \pi/2$, corresponding to a saddle-node bifurcation.

4.3. Compatibility window

We define a region in phase space where coupling dominates detuning.

Definition. Let $\bar{\phi} \in (0, \pi/2)$. Define

$$U_{\bar{\phi}} = (-\bar{\phi}, \bar{\phi}) \subset \mathbb{S}^1.$$

Boundary condition. At $\phi = \pm\bar{\phi}$,

$$|\sin\phi| = \sin\bar{\phi}.$$

If

$$|\Delta\omega| < K_{\text{tot}}(\Gamma_1, \Gamma_2)\sin\bar{\phi}, \tag{13}$$

then

$$\dot{\phi} < 0 \quad \text{at} \quad \phi = \bar{\phi},$$

and

$$\dot{\phi} > 0 \quad \text{at} \quad \phi = -\bar{\phi}.$$

Forward invariance. Under condition (13), the vector field points strictly inward at the boundary of the compatibility window. Hence the closed window

$$\overline{U}_{\bar{\phi}} = [-\bar{\phi}, \bar{\phi}]$$

is forward-invariant under the frozen dynamics. Because the boundary inequalities are strict, the open window

$$U_{\bar{\phi}} = (-\bar{\phi}, \bar{\phi})$$

is also positively invariant for trajectories that start inside it.

Relation to equilibria. If condition (13) holds, then the unique stable equilibrium ϕ^* satisfies

$$\phi^* \in U_{\bar{\phi}}.$$

Thus, under the forward-invariance condition, the stable branch lies inside the fixed compatibility window.

4.4. Threshold interpretation

We summarize the threshold conditions identified in the frozen system.

Equilibrium-existence threshold. From Section 4.1, frozen equilibria exist if

$$K_{\text{tot}}(\Gamma_1, \Gamma_2) \geq |\Delta\omega|.$$

This condition characterizes the existence of phase-locked states in the frozen system.

Compatibility-window threshold. From Section 4.3, the closed compatibility window $\overline{U}_{\bar{\phi}}$ is forward-invariant if

$$|\Delta\omega| < K_{\text{tot}}(\Gamma_1, \Gamma_2) \sin \bar{\phi}.$$

This condition ensures both the existence of a stable equilibrium and its confinement within the fixed compatibility window.

Hierarchy of conditions. These define two distinct thresholds:

$$K_{\text{tot}}(\Gamma_1, \Gamma_2) \geq |\Delta\omega| \qquad \text{existence of frozen equilibria,}$$

and

$$K_{\text{tot}}(\Gamma_1, \Gamma_2) \sin \bar{\phi} > |\Delta\omega| \qquad \text{forward invariance of } \overline{U}_{\bar{\phi}}.$$

Consequence. The second condition implies the first, since $\sin \bar{\phi} \leq 1$, and therefore provides a stronger, geometrically constrained condition on the dynamics.

Role. These thresholds characterize the frozen system and will be used in Section 5 to formulate the conditional transition from drift/traversal to capture under time-dependent coupling. In particular, the time t_c introduced in Section 5 is defined by crossing the compatibility-window threshold, rather than merely the equilibrium-existence threshold.

The distinction between equilibrium existence and forward-invariant trapping is central to the conditional accumulation-driven mechanism developed in the subsequent analysis.

5. Dynamical organization: entry, accumulation, and trapping

5.1. Fast–slow formulation and admissible integration dynamics

We consider the reduced phase dynamics of two coupled oscillators whose effective coupling is modulated by internal integration variables. The system is

$$\begin{aligned} \dot{\phi} &= \Delta\omega - K_{\text{tot}}(\Gamma_1, \Gamma_2) \sin \phi, \\ \dot{\Gamma}_i &= \varepsilon H_i(F(\phi), \Gamma_i), \qquad i = 1, 2, \end{aligned} \tag{14}$$

where $\phi \in \mathbb{S}^1$ is the phase difference, $\Delta\omega \neq 0$ is the detuning, $\Gamma_i(t) \geq 0$ are integration variables, and $0 < \varepsilon \leq \varepsilon_0$ sets the timescale separation.

We assume throughout that $\Gamma_i(0) \geq 0$ for $i = 1, 2$. By (A1), this implies $\Gamma_i(t) \geq 0$ for all t in the maximal forward interval of existence.

Notation convention for effective coupling. For notational clarity, let

$$K_{\text{tot}}(\Gamma_1, \Gamma_2)$$

denote the effective coupling as a function of the integration variables. Along trajectories of the full system, we write

$$K_{\text{tot}}(t) := K_{\text{tot}}(\Gamma_1(t), \Gamma_2(t)).$$

We use $K_{\text{tot}}(t)$ when time dependence arises through the evolution of Γ_i, and $K_{\text{tot}}(\Gamma_1, \Gamma_2)$ when referring to the mapping.

Incompatibility functional. The incompatibility functional is

$$F(\phi) = 1 - \cos\phi.$$

The specific choice $F(\phi) = 1 - \cos\phi$ ensures boundedness and non-negativity and is consistent with Assumption (A2). The growth condition on the compatibility window is imposed through (A2); the analysis extends to any phase-dependent signal satisfying the corresponding boundedness and non-negativity requirements.

Assumptions. We assume the following admissible integration–coupling structure. Throughout, we assume that $H_i(F, \Gamma_i)$ is locally Lipschitz in (F, Γ_i), and that K_{tot} satisfies the regularity condition in (A6). Hence the augmented vector field is locally Lipschitz in local charts on $\mathbb{S}^1 \times \mathbb{R}^2_+$, and solutions are locally unique.

All statements are understood on the maximal forward interval of existence. Whenever conclusions are stated for all $t \geq t_0$, they hold either globally forward in time or up to the maximal forward existence time of the corresponding solution.

(A1) Non-negativity of integration dynamics. For all $F \in [0, 2]$ and all $\Gamma_i \geq 0$,

$$H_i(F, \Gamma_i) \geq 0.$$

(A2) Positive growth inside the compatibility window. There exist $\bar{\phi} \in (0, \pi/2)$ and constants $h_i > 0$ such that

$$H_i(F(\phi), \Gamma_i) \geq h_i$$

for all

$$\phi \in U_{\bar{\phi}} \quad \text{and all} \quad \Gamma_i \geq 0,$$

where

$$U_{\bar{\phi}} = (-\bar{\phi}, \bar{\phi})$$

is the compatibility window.

(A3) Non-negative monotone coupling amplification. The map

$$K_{\text{tot}} : \mathbb{R}^2_+ \to [0, \infty)$$

is continuous and non-decreasing in each argument.

(A4) Timescale separation. There exists a fixed $\varepsilon_0 > 0$ such that

$$0 < \varepsilon \leq \varepsilon_0.$$

All $O(\varepsilon)$ estimates are understood as $\varepsilon \to 0$ on finite intervals of fixed length, with constants depending on the interval length and the bounded trajectory set under consideration, but not on ε. In the post-capture tracking result, these intervals may be shifted intervals

$$[t_*(\varepsilon), t_*(\varepsilon) + L],$$

with $L < \infty$ fixed independently of ε, provided the corresponding slow variables remain in an ε-independent compact subset of $\mathbb{R}^2_+$.

(A5) Compatibility-threshold reachability. There exists $\Gamma^* = (\Gamma_1^*, \Gamma_2^*) \in \mathbb{R}^2_+$ such that

$$|\Delta\omega| < K_{\text{tot}}(\Gamma^*) \sin\bar{\phi}.$$

Assumption (A5) is a reachability condition on the coupling function. It is not a trajectory-level crossing assumption. It only states that the coupling architecture can place the system above the compatibility-window threshold for sufficiently large integration states.

This condition concerns reachability at the level of the coupling function; trajectory-level attainment is addressed in Section 5.4 through exposure-based sufficient conditions and is not assumed to occur unconditionally.

For a fixed initial condition, Γ^* may be replaced componentwise by

$$\widehat{\Gamma}_i^* := \max\{\Gamma_i^*, \Gamma_i(0)\}, \qquad i = 1, 2.$$

By monotonicity of K_{tot}, this replacement preserves the threshold condition in (A5). Thus, the target state may be taken componentwise no smaller than the initial state.

(A6) Coupling regularity for tracking estimates. The coupling function K_{tot} extends to a C^1 function on an open neighborhood of every compact subset of $\mathbb{R}^2_+$, and its partial derivatives are locally bounded. Equivalently, for every compact set $B \subset \mathbb{R}^2_+$, there exists $C_B > 0$ such that

$$\left|\frac{\partial K_{\text{tot}}}{\partial \Gamma_i}(\Gamma)\right| \le C_B, \qquad i = 1, 2, \qquad \Gamma \in B.$$

Example: admissible integration–coupling structure. As a simple admissible example, let

$$H_i(F, \Gamma_i) = \frac{a_i}{1+F} + \rho_i \Gamma_i, \qquad a_i > 0, \quad \rho_i \ge 0,$$

and

$$K_{\text{tot}}(\Gamma_1, \Gamma_2) = K_0 + k_1\Gamma_1 + k_2\Gamma_2, \qquad k_1, k_2 > 0.$$

Since $F(\phi) = 1 - \cos\phi$ is bounded and nonnegative, there exists $F_{\max} < \infty$ such that $0 \le F(\phi) \le F_{\max}$. Hence, for $\Gamma_i \ge 0$,

$$H_i(F, \Gamma_i) \ge \frac{a_i}{1 + F_{\max}} > 0.$$

Therefore, (A1) holds, and (A2) holds with

$$h_i = \frac{a_i}{1 + F_{\max}}.$$

The function H_i is larger when F is smaller, so growth is stronger near lower-incompatibility configurations. Thus, the example aligns with compatibility-window accumulation.

The coupling K_{tot} is continuous, non-decreasing in each argument, and continuously differentiable with bounded partial derivatives, so (A3) and (A6) hold. Assumption (A4) holds by taking $0 < \varepsilon \le \varepsilon_0$, and (A5) holds for sufficiently large Γ^*.

Moreover, when at least one $\rho_i > 0$ and the corresponding coupling derivative is nonzero, the induced evolution of K_{tot} depends on the accumulated state and is not, in general, representable by a universal phase-only update law.

Remark 3 (Initial regime)**.** *We focus on initial conditions such that*

$$K_{\text{tot}}(\Gamma(0)) < |\Delta\omega|,$$

so that the system initially lies in the drift regime.

In the nontrivial accumulation case, the target configuration Γ^* *in (A5) is taken beyond the initial state, i.e.,*

$$\Gamma_i^* > \Gamma_i(0), \qquad i = 1, 2.$$

If instead

$$K_{\text{tot}}(\Gamma(0)) \ge |\Delta\omega|,$$

then the frozen phase dynamics may already possess equilibria. However, the compatibility-window trapping analysis of Sections 5.5–5.6 applies directly only once the stronger condition

$$|\Delta\omega| < K_{\text{tot}}(\Gamma(0)) \sin\bar{\phi}$$

holds.

If

$$K_{\text{tot}}(\Gamma(0)) \ge |\Delta\omega| \quad \textit{but} \quad |\Delta\omega| \ge K_{\text{tot}}(\Gamma(0)) \sin\bar{\phi},$$

then ordinary locking may occur outside the prescribed compatibility window, and window trapping still requires the compatibility-threshold condition.

Fast–slow structure. For fixed Γ_1, Γ_2, the phase equation becomes

$$\dot{\phi} = \Delta\omega - K \sin\phi, \qquad K = K_{\text{tot}}(\Gamma_1, \Gamma_2),$$

which is the classical Adler equation. It exhibits:

- drift when $K < |\Delta\omega|$;
- equilibria when $K > |\Delta\omega|$.

In the full system, however, $K_{\text{tot}}(t)$ evolves through the slow variables Γ_i, which are driven by the incompatibility functional $F(\phi)$. The resulting closed-loop cascade is

$$\phi \longrightarrow F(\phi) \longrightarrow \Gamma_i \longrightarrow K_{\text{tot}}.$$

This closed-loop cascade represents the dependence structure of the slow dynamics; the full system remains closed-loop through the feedback of K_{tot} into the phase equation.

Role of this section. This section defines the structural framework of the model, consisting of fast phase dynamics coupled to slow integration variables through a compatibility-driven cascade. Subsequent sections analyze:

- the behavior of the fast subsystem (Section 5.2);
- the traversal properties of the drift regime (Section 5.3);
- the conditions under which accumulation of the integration variables may lead to conditional threshold crossing, capture upon entry, and finite-interval tracking.

5.2. Frozen dynamics and phase structure

We analyze the fast phase dynamics with the integration variables held fixed. Fix Γ_1, Γ_2 and define

$$K := K_{\text{tot}}(\Gamma_1, \Gamma_2).$$

The frozen fast subsystem is

$$\dot{\phi} = \Delta\omega - K \sin\phi.$$

Subthreshold regime. If

$$K < |\Delta\omega|,$$

then

$$|\Delta\omega - K \sin\phi| \geq |\Delta\omega| - K > 0.$$

Thus $\dot{\phi}$ does not vanish and does not change sign. It follows that $\phi(t)$ evolves strictly monotonically and performs continuous rotations on $\mathbb{S}^1$.

Threshold regime. If $K = |\Delta\omega|$, then the equation

$$\Delta\omega = K \sin\phi$$

admits a degenerate equilibrium at

$$\phi = \operatorname{sgn}(\Delta\omega)\frac{\pi}{2} \pmod{2\pi},$$

corresponding to a saddle-node bifurcation separating drift and locking regimes.

Superthreshold regime. If

$$K > |\Delta\omega|,$$

then equilibria ϕ^* exist satisfying

$$\Delta\omega = K \sin\phi^*.$$

There are exactly two equilibria per period. The linearization is

$$\frac{d}{d\phi}\dot{\phi} = -K \cos\phi.$$

Therefore, an equilibrium ϕ^* with

$$\cos\phi^* > 0$$

is locally asymptotically stable, while an equilibrium ϕ^* with

$$\cos\phi^* < 0$$

is unstable.

Compatibility window. Let

$$U_{\bar{\phi}} = (-\bar{\phi}, \bar{\phi}), \qquad \bar{\phi} \in (0, \pi/2).$$

Within this interval, $\sin\phi$ is strictly increasing, so at most one equilibrium lies in $U_{\bar{\phi}}$.

An equilibrium lies inside the window if and only if

$$|\Delta\omega| < K \sin\bar{\phi}.$$

When this condition holds, the equilibrium belongs to $U_{\bar{\phi}}$ and is locally asymptotically stable.

Role in the full system. The frozen dynamics determine the instantaneous phase structure associated with a given value of the integration variables. As $\Gamma_i(t)$ evolve, the effective coupling $K_{\text{tot}}(t)$ changes, and the frozen system transitions between:

- a drift regime, $K < |\Delta\omega|$;
- a regime in which a stable equilibrium exists within the compatibility window, $K \sin\bar{\phi} > |\Delta\omega|$.

Subsequent sections analyze how the slow evolution of Γ_i may lead to threshold crossing. If threshold crossing occurs, the compatibility window becomes forward-invariant. Trajectories that enter this window remain captured and, on finite time intervals, track the stable phase-locked branch under the slow evolution of the coupling.

5.3. Drift regime and repeated traversal of the compatibility window

We analyze the fast subsystem in the subthreshold regime and establish the traversal properties of the phase trajectory.

Drift dynamics. Fix Γ_1, Γ_2 such that

$$K_{\text{tot}}(\Gamma_1, \Gamma_2) < |\Delta\omega|.$$

Then

$$\dot{\phi} = \Delta\omega - K_{\text{tot}} \sin\phi.$$

Since

$$|K_{\text{tot}} \sin\phi| \le K_{\text{tot}} < |\Delta\omega|,$$

it follows that

$$|\dot{\phi}| \ge |\Delta\omega| - K_{\text{tot}} > 0.$$

Thus $\dot{\phi}$ does not vanish and does not change sign, and $\phi(t)$ evolves strictly monotonically.

Moreover, there exist constants $c_-, c_+ > 0$ such that

$$0 < c_- \le |\dot{\phi}(t)| \le c_+,$$

with

$$c_- = |\Delta\omega| - K_{\text{tot}}, \qquad c_+ = |\Delta\omega| + K_{\text{tot}}.$$

On any compact uniformly subthreshold interval $[t_0, T]$ satisfying

$$K_{\text{tot}}(t) \le \overline{K} < |\Delta\omega| \qquad \text{for all } t \in [t_0, T],$$

the constants

$$c_- := |\Delta\omega| - \overline{K}, \qquad c_+ := |\Delta\omega| + \overline{K}$$

can be chosen uniformly positive.

Monotone rotation. On any subthreshold interval, we choose a continuous lift $\widetilde{\phi}(t) \in \mathbb{R}$ of the phase variable, with

$$\phi(t) = \widetilde{\phi}(t) \pmod{2\pi}.$$

Monotonicity and rotation counts are stated for this lift, with projection back to $\mathbb{S}^1$ understood modulo 2π.

If $\Delta\omega > 0$, then

$$\dot{\widetilde{\phi}} \ge \Delta\omega - K_{\text{tot}} > 0,$$

so the lift $\widetilde{\phi}(t)$ is strictly increasing. If $\Delta\omega < 0$, then

$$\dot{\widetilde{\phi}} \le \Delta\omega + K_{\text{tot}} < 0,$$

so the lift $\widetilde{\phi}(t)$ is strictly decreasing.

In both cases, the lift is strictly monotone. Since

$$\phi(t) = \widetilde{\phi}(t) \pmod{2\pi},$$

the projected trajectory on $\mathbb{S}^1$ performs rotations whenever the lift changes by 2π, and each full rotation traverses every open interval of $\mathbb{S}^1$. Full rotations are therefore counted by changes of 2π in the lift.

Traversal of the compatibility window. Let

$$U_{\bar{\phi}} = (-\bar{\phi}, \bar{\phi}).$$

We identify $U_{\bar{\phi}} \subset \mathbb{S}^1$ with the open arc around 0, represented by $(-\bar{\phi}, \bar{\phi})$ in the chart $(-\pi, \pi]$.

By a traversal of $U_{\bar{\phi}}$, we mean that the lifted trajectory crosses one full lifted copy of the arc $(-\bar{\phi}, \bar{\phi})$ modulo 2π.

Since $U_{\bar{\phi}}$ is a nonempty open subset of $\mathbb{S}^1$, every full rotation of the lifted phase trajectory produces a traversal of $U_{\bar{\phi}}$. Therefore, on any compact uniformly subthreshold interval over which the lift completes one or more full rotations, the projected trajectory traverses $U_{\bar{\phi}}$ the corresponding number of times.

Repeated traversal over an unbounded subthreshold interval follows only under an additional non-stalling condition, for example if the lift has unbounded angular displacement, or if the system remains uniformly away from the ordinary locking threshold,

$$K_{\text{tot}}(t) \le \overline{K} < |\Delta\omega|.$$

In the sequel, only the compact-interval traversal estimate below is used.

Cumulative residence time on drift intervals. Define the cumulative residence time

$$M(t) = \int_0^t \mathbf{1}_{U_{\bar{\phi}}}(\phi(s))\, ds. \tag{15}$$

Let $\ell = 2\bar{\phi}$ denote the length of $U_{\bar{\phi}}$.

On any compact uniformly subthreshold drift interval satisfying

$$K_{\mathrm{tot}}(t) \le \overline{K} < |\Delta\omega|,$$

we may choose

$$c_- := |\Delta\omega| - \overline{K}, \qquad c_+ := |\Delta\omega| + \overline{K}.$$

Then

$$0 < c_- \le |\dot{\phi}(t)| \le c_+$$

on the interval. Since $\ell = 2\bar{\phi}$, each traversal of $U_{\bar{\phi}}$ requires a time at least

$$\tau_0 := \frac{\ell}{c_+} > 0.$$

Thus, each visit contributes at least τ_0 units of time to $M(t)$.

Consequently, on any compact uniformly subthreshold drift interval during which the lifted trajectory completes repeated rotations, the cumulative residence time grows proportionally to the number of traversals.

Conclusion. On any uniformly subthreshold drift interval over which the lifted phase completes rotations, the projected trajectory traverses the compatibility window once per full rotation. Each such traversal contributes a positive residence-time contribution in $U_{\bar{\phi}}$.

Role in the mechanism. This repeated traversal provides positive residence-time contributions during intervals in which the system remains in the drift regime and completes rotations. Section 5.4 uses this property to quantify accumulation of the integration variables over such intervals, without requiring the system to remain in the drift regime for all time.

5.4. Quantified accumulation and threshold crossing condition

We quantify accumulation guaranteed by residence time in the compatibility window and establish conditions under which the compatibility-window threshold is crossed.

Compatibility-window-guaranteed growth. Let

$$U_{\bar{\phi}} = (-\bar{\phi}, \bar{\phi})$$

denote the compatibility window, and define the cumulative residence time

$$M(t) = \int_0^t \mathbf{1}_{U_{\bar{\phi}}}(\phi(s))\, ds.$$

By Assumption (A2), there exist constants $h_i > 0$ such that

$$H_i(F(\phi), \Gamma_i) \ge h_i$$

for all $\phi \in U_{\bar{\phi}}$ and all $\Gamma_i \ge 0$.

Since

$$\dot{\Gamma}_i = \varepsilon H_i(F(\phi), \Gamma_i),$$

it follows that

$$\dot{\Gamma}_i(t) \ge \varepsilon h_i\, \mathbf{1}_{U_{\bar{\phi}}}(\phi(t)).$$

Integrating over time yields the growth estimate

$$\Gamma_i(t) \geq \Gamma_i(0) + \varepsilon h_i M(t). \tag{16}$$

Compatibility-window exposure provides a guaranteed positive contribution to integration growth. Growth outside $U_{\bar{\phi}}$ is not excluded by the assumptions; the residence-time estimate uses only this guaranteed window contribution, and any additional growth can only accelerate threshold crossing.

Accumulation during the drift phase. While

$$K_{\text{tot}}(t) < |\Delta\omega|,$$

the phase dynamics are in the drift regime. By Section 5.3, the phase evolves monotonically and, over any time interval during which full rotations occur, the trajectory traverses $U_{\bar{\phi}}$ repeatedly.

Consequently, $M(t)$ is non-decreasing, and each traversal of $U_{\bar{\phi}}$ contributes a strictly positive increment to M. More generally, for any $0 \leq t_1 < t_2$,

$$\Gamma_i(t_2) - \Gamma_i(t_1) = \varepsilon \int_{t_1}^{t_2} H_i(F(\phi(s)), \Gamma_i(s))\, ds \geq \varepsilon h_i \big(M(t_2) - M(t_1)\big).$$

In particular, for any times $t_1 < t_2$ such that $M(t_2) > M(t_1)$, the integration variables satisfy

$$\Gamma_i(t_2) > \Gamma_i(t_1),$$

due to the compatibility-window growth estimate.

This argument applies to any interval during which repeated traversal occurs and does not require the system to remain in the drift regime for all time.

Persistence of coupling growth. By Assumption (A1),

$$\dot{\Gamma}_i(t) \geq 0,$$

so $\Gamma_i(t)$ are non-decreasing along trajectories. By Assumption (A3), it follows that $K_{\text{tot}}(t)$ is also non-decreasing in time.

Thus, any accumulation achieved during the drift phase is retained thereafter.

Definition of the threshold-crossing time. A threshold-crossing time is any finite time t_c such that

$$|\Delta\omega| < K_{\text{tot}}(\Gamma(t_c)) \sin\bar{\phi}. \tag{17}$$

The results below are conditional on the existence of such a time. Assumption (A5) ensures that the threshold is reachable at the level of the coupling function, while the accumulation estimates in this section provide sufficient trajectory-level conditions under which such a time exists.

Threshold crossing condition. By Assumption (A5), there exists $\Gamma^* = (\Gamma_1^*, \Gamma_2^*)$ such that

$$|\Delta\omega| < K_{\text{tot}}(\Gamma^*) \sin\bar{\phi}.$$

If there exists a finite time t_c such that

$$\Gamma_i(t_c) \geq \Gamma_i^*, \qquad i = 1, 2,$$

then, by monotonicity of K_{tot},

$$K_{\text{tot}}(\Gamma(t_c)) \geq K_{\text{tot}}(\Gamma^*),$$

and hence

$$|\Delta\omega| < K_{\text{tot}}(\Gamma(t_c)) \sin\bar{\phi}.$$

Thus, the compatibility-window threshold is crossed at time t_c.

Interpretation. The drift dynamics generate positive residence-time contribution during each traversal of the compatibility window, which drives monotone accumulation of the integration variables. This accumulation increases the effective coupling over time and may lead to threshold crossing once the accumulated state reaches a sufficiently large configuration.

Conclusion. Accumulation guaranteed by residence time in the compatibility window produces monotone growth of the integration variables and the effective coupling. Threshold crossing occurs at any finite time t_c for which the accumulated state satisfies

$$\Gamma_i(t_c) \geq \Gamma_i^*, \qquad i = 1, 2,$$

provided that sufficient compatibility-window exposure has been accumulated so that such a time exists. Assumption (A5) supplies the corresponding coupling-level reachability condition.

Lemma 1 (Subthreshold residence-time / accumulation estimate). *Let $[t_0, T]$ be a compact time interval on which the system remains in the subthreshold drift regime, and suppose that*

$$K_{\text{tot}}(t) \leq \overline{K} < |\Delta\omega| \qquad \textit{for all } t \in [t_0, T].$$

Define

$$c_- := |\Delta\omega| - \overline{K}, \qquad c_+ := |\Delta\omega| + \overline{K}.$$

Then

$$0 < c_- \leq |\dot{\phi}(t)| \leq c_+ \qquad \textit{for all } t \in [t_0, T].$$

Let $\widetilde{\phi}(t)$ be a continuous lift of $\phi(t)$ on $[t_0, T]$, and define the lifted compatibility window by

$$\widetilde{U}_{\bar{\phi}} := \bigcup_{m \in \mathbb{Z}} (2\pi m - \bar{\phi},\, 2\pi m + \bar{\phi}) \subset \mathbb{R}.$$

Then

$$M(T) - M(t_0) \geq \frac{2\bar{\phi}}{c_+} \left\lfloor \frac{c_-(T - t_0)}{2\pi} \right\rfloor. \tag{18}$$

Consequently,

$$\Gamma_i(T) \geq \Gamma_i(t_0) + \varepsilon h_i \frac{2\bar{\phi}}{c_+} \left\lfloor \frac{c_-(T - t_0)}{2\pi} \right\rfloor, \qquad i = 1, 2. \tag{19}$$

Proof. The velocity bounds follow from

$$|\dot{\phi}(t)| = |\Delta\omega - K_{\text{tot}}(t) \sin\phi(t)| \geq |\Delta\omega| - K_{\text{tot}}(t) \geq c_-,$$

and

$$|\dot{\phi}(t)| \leq |\Delta\omega| + K_{\text{tot}}(t) \leq c_+.$$

Let $\widetilde{I} \subset \mathbb{R}$ denote the interval between $\widetilde{\phi}(t_0)$ and $\widetilde{\phi}(T)$. Since the lift is monotone on $[t_0, T]$, and since $|\dot{\widetilde{\phi}}(t)| \leq c_+$, the change-of-variables estimate gives

$$M(T) - M(t_0) = \int_{t_0}^{T} \mathbf{1}_{U_{\bar{\phi}}}(\phi(t))\, dt \geq \frac{1}{c_+} \int_{\widetilde{I}} \mathbf{1}_{\widetilde{U}_{\bar{\phi}}}(\theta)\, d\theta.$$

The set $\widetilde{U}_{\bar{\phi}}$ is 2π-periodic, and every interval of length 2π contains exactly $2\bar{\phi}$ units of $\widetilde{U}_{\bar{\phi}}$-measure. Moreover, the interval $\widetilde{I}$ contains at least

$$\left\lfloor \frac{|\widetilde{\phi}(T) - \widetilde{\phi}(t_0)|}{2\pi} \right\rfloor$$

full disjoint subintervals of length 2π. Therefore,

$$\int_{\widetilde{I}} \mathbf{1}_{\widetilde{U}_{\bar{\phi}}}(\theta)\, d\theta \geq 2\bar{\phi} \left\lfloor \frac{|\widetilde{\phi}(T) - \widetilde{\phi}(t_0)|}{2\pi} \right\rfloor.$$

Hence,

$$M(T) - M(t_0) \geq \frac{2\bar{\phi}}{c_+} \left\lfloor \frac{|\widetilde{\phi}(T) - \widetilde{\phi}(t_0)|}{2\pi} \right\rfloor.$$

Moreover, since $|\dot{\widetilde{\phi}}(t)| \geq c_-$ on $[t_0, T]$,

$$|\widetilde{\phi}(T) - \widetilde{\phi}(t_0)| \geq c_-(T - t_0),$$

which gives (18). Combining this with the growth estimate (16) gives (19). □

This estimate quantifies accumulation during compact uniformly subthreshold drift intervals. It does not, by itself, imply crossing of the compatibility-window threshold, since that threshold lies above the ordinary drift-locking threshold $K_{\text{tot}} = |\Delta\omega|$.

Lemma 2 (Exposure-based conditional crossing)**.** *Let $T > 0$ be a finite time such that the solution exists on $[0, T]$. Suppose that*

$$M(T) \geq \max_{i=1,2} \frac{(\Gamma_i^* - \Gamma_i(0))_+}{\varepsilon h_i}, \qquad (x)_+ := \max\{x, 0\}. \tag{20}$$

Then

$$\Gamma_i(T) \geq \Gamma_i^*, \qquad i = 1, 2.$$

Consequently, by Assumptions (A3)–(A5),

$$|\Delta\omega| < K_{\text{tot}}(\Gamma(T)) \sin\bar{\phi}.$$

Thus, sufficient accumulated exposure implies the compatibility-window threshold condition at time T.

Proof. By (16),

$$\Gamma_i(T) \geq \Gamma_i(0) + \varepsilon h_i M(T).$$

Using (20), we obtain

$$\Gamma_i(T) \geq \Gamma_i(0) + (\Gamma_i^* - \Gamma_i(0))_+ \geq \Gamma_i^*, \qquad i = 1, 2.$$

The threshold conclusion follows from the monotonicity of K_{tot} and Assumption (A5). □

5.5. Threshold-induced forward invariance and capture

We show that whenever the effective coupling crosses the compatibility-window threshold, the compatibility window becomes forward-invariant, and trajectories that enter the window remain trapped.

Threshold time. From Section 5.4, suppose there exists a finite time t_c such that

$$|\Delta\omega| < K_{\text{tot}}(t_c) \sin\bar{\phi}.$$

Since the integration variables $\Gamma_i(t)$ are non-decreasing by (A1), and K_{tot} is non-decreasing in each argument by (A3), it follows that

$$|\Delta\omega| < K_{\text{tot}}(t) \sin\bar{\phi} \qquad \text{for all } t \geq t_c, \quad t \in I_{\max}.$$

Forward invariance of the closed compatibility window. Let

$$\overline{U}_{\bar{\phi}} := [-\bar{\phi}, \bar{\phi}], \qquad U_{\bar{\phi}} = (-\bar{\phi}, \bar{\phi}).$$

Whenever barrier arguments are applied to this interval, we use the real representative of $\mathbb{S}^1$ in the chart $(-\pi, \pi]$, so that $\overline{U}_{\bar{\phi}}$ has boundary points $\pm\bar{\phi}$.

Since the threshold inequality is strict at t_c, define

$$\eta_c := K_{\text{tot}}(t_c) \sin\bar{\phi} - |\Delta\omega| > 0.$$

By monotonicity of the integration variables and of K_{tot},

$$K_{\text{tot}}(t)\sin\bar{\phi} - |\Delta\omega| \geq \eta_c \qquad \text{for all } t \geq t_c, \quad t \in I_{\max}.$$

The phase dynamics are

$$\dot{\phi} = \Delta\omega - K_{\text{tot}}(t)\sin\phi.$$

At the boundary $\phi = \bar{\phi}$,

$$\dot{\phi} = \Delta\omega - K_{\text{tot}}(t)\sin\bar{\phi} \leq |\Delta\omega| - K_{\text{tot}}(t)\sin\bar{\phi} \leq -\eta_c < 0.$$

At the boundary $\phi = -\bar{\phi}$,

$$\dot{\phi} = \Delta\omega + K_{\text{tot}}(t)\sin\bar{\phi} \geq -|\Delta\omega| + K_{\text{tot}}(t)\sin\bar{\phi} \geq \eta_c > 0.$$

Thus, for all $t \geq t_c$ with $t \in I_{\max}$, the vector field points strictly inward at both boundary points of $\overline{U}_{\bar{\phi}}$. If a trajectory starting in $\overline{U}_{\bar{\phi}}$ were to exit the interval within $I_{\max}$, there would be a first exit time at one of the boundary points. The inward-pointing inequalities at both boundary points contradict the outward derivative required at such a first exit time. Hence, by the standard scalar barrier argument, the closed interval $\overline{U}_{\bar{\phi}} = [-\bar{\phi}, \bar{\phi}]$ is positively invariant for the non-autonomous system.

Because the inward inequalities are strict, a trajectory starting in the open interval $U_{\bar{\phi}} = (-\bar{\phi}, \bar{\phi})$ cannot reach either boundary in forward time within $I_{\max}$. Hence the open window is positively invariant for post-threshold trajectories that enter it. It follows that

$$\phi(t_0) \in U_{\bar{\phi}}, \quad t_0 \geq t_c \quad \Longrightarrow \quad \phi(t) \in U_{\bar{\phi}} \quad \text{for all } t \geq t_0, \quad t \in I_{\max}. \tag{21}$$

Capture upon entry into the compatibility window. Assume that $\phi(t_c) \notin U_{\bar{\phi}}$ and consider the trajectory for $t \geq t_c$. If the trajectory enters $U_{\bar{\phi}}$ at some time $t_* \geq t_c$, then by forward invariance it remains in $U_{\bar{\phi}}$ for all subsequent time:

$$\phi(t) \in U_{\bar{\phi}} \qquad \text{for all } t \geq t_*, \quad t \in I_{\max}.$$

Thus, once entry occurs, the trajectory is captured and cannot exit the compatibility window for later times in $I_{\max}$.

For the corresponding frozen system, phase-line analysis shows that the stable equilibrium lies inside the compatibility window once

$$K\sin\bar{\phi} > |\Delta\omega|.$$

This frozen-system observation motivates the capture mechanism. In the full non-autonomous system, however, finite-time entry is not asserted without an additional hypothesis; the theorem assumes the existence of an entry time $t_* \geq t_c$.

Conclusion. Once the compatibility threshold is crossed, the compatibility window becomes forward-invariant. Any trajectory entering the window after threshold crossing is captured for all later times in $I_{\max}$, and the post-capture tracking estimate applies from the entry time onward.

5.6. Post-capture stability and finite-interval tracking

We describe the phase dynamics after threshold crossing and capture within the compatibility window.

Post-capture regime. Consider trajectories for which there exists a time $t_* \geq t_c$ such that

$$\phi(t_*) \in U_{\bar{\phi}}.$$

By Section 5.5, it follows that

$$\phi(t) \in U_{\bar{\phi}} \qquad \text{for all } t \geq t_*, \quad t \in I_{\max}.$$

For all $t \geq t_c$ with $t \in I_{\max}$,

$$|\Delta\omega| < K_{\text{tot}}(t)\sin\bar{\phi}.$$

Thus, for each fixed $t \geq t_*$, the frozen subsystem

$$\dot{\phi} = \Delta\omega - K_{\text{tot}}(t)\sin\phi$$

admits a unique stable equilibrium $\phi^*(t) \in U_{\bar{\phi}}$. In the full non-autonomous system, $\phi^*(t)$ is understood as a moving frozen equilibrium branch rather than a stationary solution.

Explicitly,

$$\phi^*(t) = \arcsin\left(\frac{\Delta\omega}{K_{\text{tot}}(t)}\right), \tag{22}$$

where arcsin is taken on the principal branch with values in $(-\pi/2, \pi/2)$. Equivalently,

$$\Delta\omega = K_{\text{tot}}(t) \sin\phi^*(t).$$

Uniform stability. The linearization at $\phi^*(t)$ is

$$\frac{d}{d\phi}\dot{\phi} = -K_{\text{tot}}(t)\cos\phi.$$

Since $\phi^*(t) \in (-\bar{\phi}, \bar{\phi}) \subset (-\pi/2, \pi/2)$,

$$\cos\phi^*(t) \geq \cos\bar{\phi} > 0.$$

Moreover, since the compatibility-window threshold persists for $t \geq t_c$,

$$|\Delta\omega| < K_{\text{tot}}(t)\sin\bar{\phi}.$$

Define the uniform contraction rate

$$\lambda_0 := |\Delta\omega| \cot\bar{\phi} > 0. \tag{23}$$

Then, for all $t \geq t_c$ with $t \in I_{\max}$,

$$K_{\text{tot}}(t)\cos\bar{\phi} \geq \lambda_0.$$

Hence,

$$\frac{d}{d\phi}\dot{\phi}\big(\phi^*(t)\big) = -K_{\text{tot}}(t)\cos\phi^*(t) \leq -\lambda_0.$$

Thus, the frozen equilibrium branch is uniformly linearly attracting. Moreover, for points in the captured window, the mean-value estimate below gives a uniform one-sided contraction bound with rate at least λ_0.

Error dynamics. After capture, we use the real representative of $\phi(t)$ in $U_{\bar{\phi}}$, so that the difference $e(t) = \phi(t) - \phi^*(t)$ is well-defined. Let

$$e(t) := \phi(t) - \phi^*(t), \qquad V(t) := \frac{1}{2}e(t)^2.$$

Then

$$\dot{e} = \dot{\phi} - \dot{\phi}^*.$$

Using

$$\dot{\phi} = \Delta\omega - K_{\text{tot}}(t)\sin\phi, \qquad \Delta\omega = K_{\text{tot}}(t)\sin\phi^*(t),$$

we obtain

$$\dot{e} = -K_{\text{tot}}(t)\big(\sin\phi - \sin\phi^*(t)\big) - \dot{\phi}^*(t).$$

By the mean value theorem,

$$\sin\phi - \sin\phi^*(t) = \cos\xi(t)\, e(t),$$

for some $\xi(t)$ between $\phi(t)$ and $\phi^*(t)$. Since both lie in $U_{\bar{\phi}}$,

$$\cos\xi(t) \geq \cos\bar{\phi}.$$

Thus,

$$\dot{V} \leq -K_{\text{tot}}(t)\cos\bar{\phi}\, e^2 + |e|\,|\dot{\phi}^*(t)|.$$

Since

$$K_{\text{tot}}(t)\cos\bar{\phi} \geq \lambda_0 \qquad \text{for all } t \geq t_c, \quad t \in I_{\max},$$

and $e^2 = 2V$, we obtain

$$\dot{V} \leq -2\lambda_0 V + |e|\,|\dot{\phi}^*(t)|.$$

Slow variation of the equilibrium. Fix a finite post-capture interval $[t_*, t_* + L] \subset I_{\max}$, where $L < \infty$ is fixed independently of ε, and suppose that the corresponding family of captured trajectories $\Gamma(t)$ remains in an ε-independent compact subset of $\mathbb{R}^2_+$ on this interval.

Since F is bounded and H_i is locally bounded, there exists a constant $C > 0$, independent of ε, such that

$$|H_i(F(\phi(t)), \Gamma_i(t))| \le C, \qquad t \in [t_*, t_* + L].$$

Therefore,

$$|\dot{\Gamma}_i(t)| = \varepsilon |H_i(F(\phi(t)), \Gamma_i(t))| \le C\varepsilon,$$

so

$$\dot{\Gamma}_i(t) = O(\varepsilon)$$

on $[t_*, t_* + L]$, with constants independent of ε.

By (A6), K_{tot} is C^1 on a neighborhood of this compact set, with partial derivatives bounded on the compact set. Therefore,

$$\dot{K}_{\text{tot}}(t) = \sum_i \frac{\partial K_{\text{tot}}}{\partial \Gamma_i}(\Gamma(t))\dot{\Gamma}_i(t) = O(\varepsilon)$$

on $[t_*, t_* + L]$, with constants independent of ε.

Since $\Gamma(t)$ is C^1 and K_{tot} is C^1 on a neighborhood of the compact set containing $\Gamma(t)$, it follows that $K_{\text{tot}}(t) = K_{\text{tot}}(\Gamma(t))$ is C^1 on the post-capture interval. Moreover, because the branch $\phi^*(t)$ is defined by (22), with arcsin taken on the principal branch, $\phi^*(t)$ is C^1 on the interval as well.

Differentiating

$$\Delta\omega = K_{\text{tot}}(t) \sin \phi^*(t)$$

gives

$$0 = \dot{K}_{\text{tot}}(t) \sin \phi^*(t) + K_{\text{tot}}(t) \cos \phi^*(t) \dot{\phi}^*(t).$$

Hence,

$$\dot{\phi}^*(t) = -\frac{\dot{K}_{\text{tot}}(t)}{K_{\text{tot}}(t)} \tan \phi^*(t).$$

Since $\phi^*(t) \in U_{\bar{\phi}}$, we have

$$|\tan \phi^*(t)| \le C_0.$$

Since

$$K_{\text{tot}}(t) > \frac{|\Delta\omega|}{\sin \bar{\phi}}$$

for all $t \ge t_c$, $K_{\text{tot}}(t)$ is bounded away from zero uniformly on the post-threshold interval. Together with $\dot{K}_{\text{tot}}(t) = O(\varepsilon)$, this gives a constant $C > 0$, independent of ε, such that

$$|\dot{\phi}^*(t)| \le C\varepsilon, \qquad t \in [t_*, t_* + L].$$

Tracking estimate. The $O(\varepsilon)$ estimates are interpreted for families of captured solutions indexed by ε, on finite post-capture intervals whose slow variables remain in an ε-independent compact set.

The following tracking estimate is understood on every finite post-capture interval $[t_*, t_* + L] \subset I_{\max}$, where $L < \infty$ is fixed independently of ε, and on which the corresponding family of captured trajectories $\Gamma(t)$ remains in an ε-independent compact subset of $\mathbb{R}^2_+$. The constant C_L may depend on this compact set and on L, but not on ε.

Using the bound above,

$$\dot{V} \le -2\lambda_0 V + C\varepsilon|e| \le -\lambda_0 V + C'\varepsilon^2.$$

By Grönwall's inequality,

$$V(t) \le e^{-\lambda_0(t-t_*)} V(t_*) + C_L \varepsilon^2, \qquad t \in [t_*, t_* + L] \subset I_{\max}.$$

Therefore,

$$|e(t)| \le e^{-\lambda_0(t-t_*)/2} |e(t_*)| + C_L \varepsilon, \qquad t \in [t_*, t_* + L] \subset I_{\max}.$$

Equivalently,

$$|\phi(t) - \phi^*(t)| \leq e^{-\lambda_0(t-t_*)/2}|\phi(t_*) - \phi^*(t_*)| + C_L\varepsilon, \qquad t \in [t_*, t_* + L] \subset I_{\max}. \tag{24}$$

In particular, if

$$|\phi(t_*) - \phi^*(t_*)| = O(\varepsilon),$$

then

$$\phi(t) = \phi^*(t) + O(\varepsilon)$$

on $[t_*, t_* + L] \subset I_{\max}$.

More generally, on such finite post-capture intervals, captured trajectories satisfy a stability estimate consisting of an exponentially decaying entry-error term plus an $O(\varepsilon)$ forcing term; full $O(\varepsilon)$ tracking follows whenever the entry error is $O(\varepsilon)$.

Asymptotic alignment. From

$$\sin\phi^*(t) = \frac{\Delta\omega}{K_{\text{tot}}(t)},$$

it follows that if

$$K_{\text{tot}}(t) \to \infty,$$

then

$$\phi^*(t) \to 0.$$

This statement concerns the moving frozen equilibrium branch; the actual captured trajectory follows it according to the finite-interval tracking estimate above.

Conclusion. After capture, the dynamics are governed by uniform contraction toward a slowly varying frozen equilibrium branch. On finite post-capture intervals of length L fixed independently of ε, captured trajectories satisfy a stability estimate consisting of an exponentially decaying entry-error term plus an $O(\varepsilon)$ forcing term; full $O(\varepsilon)$ tracking follows whenever the entry error is $O(\varepsilon)$.

5.7. Non-reducibility to phase-only adaptive coupling laws

We show that, under genuine hidden-state dependence, the induced coupling evolution cannot in general be represented by a universal phase-only adaptive law of the form

$$\dot{K} = f(\phi)$$

without introducing additional state variables. This result does not exclude scalar adaptive laws with explicit K-dependence, such as

$$\dot{K} = g(\phi, K),$$

nor higher-dimensional adaptive closures.

Direct adaptive coupling. In standard adaptive formulations, the evolution of the coupling is given by

$$\dot{K} = f(\phi),$$

where f depends only on the instantaneous phase difference. Such laws are phase-only at the level of the update rule: for a given instantaneous phase value ϕ, the coupling derivative $\dot{K}$ is fixed independently of any additional hidden integration state.

Compatibility–integration coupling. In the present framework, the coupling evolves through the cascade

$$\phi \longrightarrow F(\phi) \longrightarrow \Gamma_i \longrightarrow K_{\text{tot}},$$

with

$$\dot{\Gamma}_i = \varepsilon H_i(F(\phi), \Gamma_i),$$

and K_{tot} non-decreasing in each Γ_i. Thus, $K_{\text{tot}}(t)$ depends on the internal variables $\Gamma_i(t)$, and therefore on the accumulated history of the trajectory $\phi(s)$ for $s \leq t$.

History dependence. Let $\phi_1(t)$ and $\phi_2(t)$ be two trajectories such that

$$\phi_1(t_0) = \phi_2(t_0),$$

but with different histories prior to t_0. Then, in general,

$$\Gamma_i^{(1)}(t_0) \neq \Gamma_i^{(2)}(t_0), \qquad K_{\mathrm{tot}}^{(1)}(t_0) \neq K_{\mathrm{tot}}^{(2)}(t_0).$$

For phase values satisfying

$$\sin\phi(t_0) \neq 0,$$

these different coupling values generally induce different phase velocities. More importantly for the present non-reducibility claim, the induced coupling derivatives may differ at the same instantaneous phase value.

Thus, the vector field of the reduced phase equation is not, in general, a function of ϕ alone, but depends on additional state variables encoding accumulated history. In particular, the dynamics are not Markovian when projected onto the ϕ-coordinate alone.

Proposition 1 (Non-reducibility under genuine hidden-state dependence)**.** *We call the integration–coupling structure genuinely hidden-state dependent if there exist two admissible augmented states (ϕ, Γ) and $(\phi, \widetilde{\Gamma})$, with the same phase value ϕ, such that the induced coupling derivatives are different:*

$$\sum_i \frac{\partial K_{\mathrm{tot}}}{\partial \Gamma_i}(\Gamma) H_i(F(\phi), \Gamma_i) \neq \sum_i \frac{\partial K_{\mathrm{tot}}}{\partial \Gamma_i}(\widetilde{\Gamma}) H_i(F(\phi), \widetilde{\Gamma}_i). \tag{25}$$

Here, admissible augmented states mean states in the phase–integration state space that may be used as initial data for the augmented system. The common positive factor ε is omitted from this comparison.

Under this nondegeneracy condition, no phase-only adaptive law of the form

$$\dot{K} = f(\phi)$$

can reproduce the induced coupling evolution of the full augmented system for all admissible histories.

Proof. Suppose for contradiction that such a representation exists. Then there would be a single function $f : \mathbb{S}^1 \to \mathbb{R}$ such that

$$\dot{K}_{\mathrm{tot}}(t) = f(\phi(t))$$

along all admissible histories of the augmented system.

In particular, for any two admissible trajectories satisfying

$$\phi_1(t_0) = \phi_2(t_0),$$

one must have

$$\dot{K}_{\mathrm{tot}}^{(1)}(t_0) = \dot{K}_{\mathrm{tot}}^{(2)}(t_0),$$

because the right-hand side depends only on the instantaneous phase value.

However, in the present system,

$$\dot{K}_{\mathrm{tot}}(t) = \sum_i \frac{\partial K_{\mathrm{tot}}}{\partial \Gamma_i}(\Gamma(t))\dot{\Gamma}_i(t) = \varepsilon \sum_i \frac{\partial K_{\mathrm{tot}}}{\partial \Gamma_i}(\Gamma(t)) H_i(F(\phi(t)), \Gamma_i(t)).$$

By genuine hidden-state dependence, the induced value of $\dot{K}_{\mathrm{tot}}$ depends genuinely on the hidden integration state Γ at fixed ϕ. Thus, two admissible augmented states with the same instantaneous phase value may induce different values of $\dot{K}_{\mathrm{tot}}$.

This contradicts the existence of a universal phase-only representation $\dot{K} = f(\phi)$ capable of reproducing the trajectory-dependent coupling evolution of the full augmented system for all admissible histories. □

This result does not exclude adaptive laws depending on additional variables, nor laws of the form

$$\dot{K} = g(\phi, K).$$

It only excludes universal representation by phase-only update laws $\dot{K} = f(\phi)$ when $\dot{K}_{\mathrm{tot}}$ depends genuinely on hidden integration states at fixed phase. This proposition is not used in the proof of Theorem 1; its role is structural.

Dynamical consequence. The non-reducibility has direct dynamical implications. The mechanism established in Sections 5.3–5.6 relies on:

- repeated traversal of the compatibility window;
- cumulative accumulation of integration variables;
- conditional threshold crossing;
- formation of a forward-invariant trapping region;
- capture upon entry and finite-interval tracking of the moving frozen equilibrium branch.

This behavior arises from the dependence of the coupling on accumulated compatibility. Although phase-only adaptive laws $\dot{K} = f(\phi)$ may themselves accumulate through the scalar state $K(t)$, they cannot reproduce the full augmented trajectory family of the present model under genuine hidden-state dependence.

Conclusion. The compatibility–integration architecture defines a class of adaptive coupling systems with intrinsic memory, in which the effective coupling depends on accumulated compatibility rather than instantaneous phase difference.

Consequently, under genuine hidden-state dependence, phase-only adaptive coupling laws of the form $\dot{K} = f(\phi)$ cannot reproduce the full augmented trajectory family of the present model. We emphasize that this non-reducibility result concerns phase-only adaptive laws; the full system remains Markovian on the augmented state space $(\phi, \Gamma_1, \Gamma_2)$.

5.8. Theorem—Conditional exposure-driven threshold crossing, capture, and finite-interval tracking

Theorem 1 (Conditional exposure-driven threshold crossing, capture, and finite-interval tracking)**.** *Consider the system*

$$\dot{\phi} = \Delta\omega - K_{\mathrm{tot}}(\Gamma_1, \Gamma_2)\sin\phi, \qquad \dot{\Gamma}_i = \varepsilon H_i(F(\phi), \Gamma_i), \qquad i = 1, 2,$$

with

$$F(\phi) = 1 - \cos\phi,$$

$0 < \varepsilon \le \varepsilon_0$, *and assumptions (A1)–(A6). Let*

$$U_{\bar{\phi}} = (-\bar{\phi}, \bar{\phi}), \qquad \bar{\phi} \in (0, \pi/2).$$

For the fixed initial condition under consideration, replace Γ^*, *if necessary, by the componentwise enlarged target*

$$\widehat{\Gamma}_i^* := \max\{\Gamma_i^*, \Gamma_i(0)\}, \qquad i = 1, 2.$$

By monotonicity of K_{tot}, *this replacement preserves the compatibility-threshold condition in (A5). For notational simplicity, we again denote the enlarged target by* Γ^*.

Let

$$I_{\max} = [0, T_{\max})$$

denote the maximal forward interval of existence of the corresponding solution. All statements involving $t \ge t_c$ *or* $t \ge t_*$ *are understood for* $t \in I_{\max}$.

Then the following statements hold.

(i) ***Drift and traversal.*** *On any interval over which*

$$K_{\mathrm{tot}}(t) < |\Delta\omega|,$$

choose a continuous lift $\widetilde{\phi}(t) \in \mathbb{R}$ *of the phase variable, with*

$$\phi(t) = \widetilde{\phi}(t) \pmod{2\pi}.$$

The lift $\widetilde{\phi}(t)$ *evolves monotonically.*

On compact subthreshold intervals satisfying

$$K_{\text{tot}}(t) \le \overline{K} < |\Delta\omega|,$$

the rotation and residence-time estimates hold uniformly. During such intervals, the projected trajectory on $\mathbb{S}^1$ *traverses* $U_{\bar{\phi}}$ *whenever the lift completes a full rotation. Here, a full rotation means an interval over which the lift* $\widetilde{\phi}(t)$ *changes by at least* 2π.

(ii) ***Compatibility exposure.*** *Let*

$$M(t) = \int_0^t \mathbf{1}_{U_{\bar{\phi}}}(\phi(s))\, ds.$$

While the trajectory remains in the subthreshold drift regime and performs repeated traversals of $U_{\bar{\phi}}$, *the quantity* $M(t)$ *increases by a strictly positive amount during each traversal. In particular,* $M(t)$ *is non-decreasing, and each traversal of* $U_{\bar{\phi}}$ *contributes a strictly positive increment to* M.

(iii) ***Integration growth.*** *There exist constants* $h_i > 0$ *such that*

$$\Gamma_i(t) \ge \Gamma_i(0) + \varepsilon h_i M(t).$$

(iv) ***Threshold crossing condition.*** *Let* $\Gamma^* = (\Gamma_1^*, \Gamma_2^*)$ *be as in (A5). If there exists a finite time* t_c *such that*

$$M(t_c) \ge \max_{i=1,2} \frac{(\Gamma_i^* - \Gamma_i(0))_+}{\varepsilon h_i}, \qquad (x)_+ := \max\{x, 0\}, \tag{26}$$

then

$$\Gamma_i(t_c) \ge \Gamma_i^*, \qquad i = 1, 2.$$

Consequently, by monotonicity of K_{tot} *and by (A5),*

$$|\Delta\omega| < K_{\text{tot}}(\Gamma(t_c)) \sin\bar{\phi}.$$

Thus, sufficient accumulated compatibility-window exposure implies crossing of the compatibility-window threshold. Equivalently, the same conclusion holds whenever

$$\Gamma_i(t_c) \ge \Gamma_i^*, \qquad i = 1, 2.$$

(v) ***Forward invariance.*** *If the threshold condition in* (iv) *holds at time* t_c, *then for all* $t \ge t_c$ *with* $t \in I_{\max}$, *the closed interval*

$$\overline{U}_{\bar{\phi}} := [-\bar{\phi}, \bar{\phi}]$$

is positively invariant for the non-autonomous phase dynamics.
Consequently, any trajectory entering

$$U_{\bar{\phi}} = (-\bar{\phi}, \bar{\phi})$$

at a time $t_* \ge t_c$ *remains in* $U_{\bar{\phi}}$ *for all later times in* $I_{\max}$.

(vi) ***Capture upon entry.*** *If the threshold condition holds and there exists a time* $t_* \ge t_c$ *such that*

$$\phi(t_*) \in U_{\bar{\phi}},$$

then

$$\phi(t) \in U_{\bar{\phi}} \qquad \text{for all } t \ge t_*, \quad t \in I_{\max}.$$

Thus, entry into the compatibility window after threshold crossing implies capture for all later times in $I_{\max}$.

(vii) ***Locking and tracking.*** *Assume the threshold condition in* (iv) *holds at time* t_c, *and assume there exists* $t_* \ge t_c$ *such that*

$$\phi(t_*) \in U_{\bar{\phi}}.$$

The times $t_c = t_c(\varepsilon)$ *and* $t_* = t_*(\varepsilon)$ *may depend on* ε. *The tracking estimate is asserted only on shifted finite intervals*

$$[t_*, t_* + L] \subset I_{\max},$$

with $L < \infty$ fixed independently of ε.
For $t \geq t_*$, let $\phi^*(t) \in U_{\bar{\phi}}$ be the unique stable frozen equilibrium branch given by

$$\phi^*(t) = \arcsin\left(\frac{\Delta\omega}{K_{\mathrm{tot}}(t)}\right),$$

where arcsin *is taken on the principal branch with values in $(-\pi/2, \pi/2)$. Equivalently,*

$$\Delta\omega = K_{\mathrm{tot}}(t)\sin\phi^*(t).$$

Define

$$\lambda_0 := |\Delta\omega| \cot\bar{\phi} > 0.$$

Since the threshold condition persists for $t \geq t_c$,

$$|\Delta\omega| < K_{\mathrm{tot}}(t)\sin\bar{\phi},$$

and therefore

$$K_{\mathrm{tot}}(t)\cos\bar{\phi} \geq \lambda_0 \qquad \text{for all } t \geq t_c.$$

On every finite post-capture interval $[t_*, t_* + L] \subset I_{\max}$, where $L < \infty$ is fixed independently of ε, and on which the corresponding family of captured trajectories $\Gamma(t)$ remains in an ε-independent compact subset of $\mathbb{R}^2_+$, there exists a constant $C_L > 0$, depending on this compact set and on L, but not on ε, such that

$$|\phi(t) - \phi^*(t)| \leq e^{-\lambda_0(t-t_*)/2}|\phi(t_*) - \phi^*(t_*)| + C_L\varepsilon, \qquad t \in [t_*, t_* + L] \subset I_{\max}. \tag{27}$$

If, in addition,

$$|\phi(t_*) - \phi^*(t_*)| = O(\varepsilon),$$

then

$$\phi(t) = \phi^*(t) + O(\varepsilon)$$

on $[t_*, t_* + L] \subset I_{\max}$.
Thus, on such finite post-capture intervals, captured trajectories satisfy a stability estimate consisting of an exponentially decaying entry-error term plus an $O(\varepsilon)$ forcing term; full $O(\varepsilon)$ tracking follows whenever the entry error is $O(\varepsilon)$.
Moreover, along trajectories for which $K_{\mathrm{tot}}(t)$ grows without bound,

$$\phi^*(t) \to 0.$$

The accumulation estimate of Section 5.4 quantifies growth on compact subthreshold drift intervals. Since the compatibility-window threshold

$$K_{\mathrm{tot}}\sin\bar{\phi} > |\Delta\omega|$$

lies above the ordinary drift-locking threshold

$$K_{\mathrm{tot}} = |\Delta\omega|,$$

this estimate alone does not imply unconditional finite-time crossing of the compatibility-window threshold. The capture and tracking results are therefore stated conditionally on the existence of a finite threshold-crossing time, or whenever a separately verified trajectory-level estimate establishes such a time.

Summary.

drift/traversal $\Longrightarrow$ exposure-driven accumulation
$\Longrightarrow$ threshold crossing when sufficient exposure is attained
$\Longrightarrow$ capture upon post-threshold entry $\Longrightarrow$ finite-interval tracking.

5.9. Proof of accumulation-driven capture and locking

We prove each part of Theorem 1 in sequence.

Proof of (i): Drift and traversal. Consider any compact subthreshold interval $I = [t_0, T]$ on which

$$K_{\text{tot}}(t) \le \overline{K} < |\Delta\omega|.$$

Choose a continuous lift $\widetilde{\phi}(t) \in \mathbb{R}$ of the phase variable on I, with

$$\phi(t) = \widetilde{\phi}(t) \pmod{2\pi}.$$

Define

$$c_- := |\Delta\omega| - \overline{K} > 0.$$

Then, for $t \in I$,

$$|\dot{\widetilde{\phi}}(t)| = |\Delta\omega - K_{\text{tot}}(t)\sin\phi(t)| \ge |\Delta\omega| - K_{\text{tot}}(t) \ge |\Delta\omega| - \overline{K} = c_-.$$

Thus $\dot{\widetilde{\phi}}$ does not vanish on I and does not change sign while the trajectory remains in the subthreshold drift regime. Hence the lift $\widetilde{\phi}(t)$ evolves monotonically over such intervals.

Since $|\dot{\widetilde{\phi}}| \ge c_- > 0$ on such an interval, any subinterval on which the lift changes by at least 2π corresponds to a full rotation of the projected trajectory on $\mathbb{S}^1$. During each full rotation, the projected trajectory traverses every open interval of $\mathbb{S}^1$, including $U_{\bar{\phi}}$.

Consequently, during compact subthreshold drift intervals in which full rotations occur, the projected trajectory traverses every open interval of $\mathbb{S}^1$, including $U_{\bar{\phi}}$, repeatedly. □

Proof of (ii): Compatibility exposure. Consider any compact subthreshold interval $I = [t_0, T]$ on which

$$K_{\text{tot}}(t) \le \overline{K} < |\Delta\omega|.$$

Then, as in Section 5.3, there exist constants $c_-, c_+ > 0$ such that

$$0 < c_- \le |\dot{\phi}(t)| \le c_+, \qquad t \in I.$$

Each traversal of $U_{\bar{\phi}}$, which has length $2\bar{\phi}$, requires a time at least

$$\tau_0 = \frac{2\bar{\phi}}{c_+} > 0.$$

During any compact subthreshold interval in which the trajectory performs repeated traversals of $U_{\bar{\phi}}$, each traversal contributes at least τ_0 to the cumulative residence time $M(t)$.

Hence, on such intervals, $M(t)$ is non-decreasing, and each traversal contributes a strictly positive increment to M. The quantitative lower bound on residence time is given by the lifted-measure estimate in Section 5.4. □

Proof of (iii): Integration growth. By (A2),

$$H_i(F(\phi), \Gamma_i) \ge h_i \qquad \text{for } \phi \in U_{\bar{\phi}}.$$

Thus

$$\dot{\Gamma}_i(t) \ge \varepsilon h_i \mathbf{1}_{U_{\bar{\phi}}}(\phi(t)).$$

Integrating,

$$\Gamma_i(t) \ge \Gamma_i(0) + \varepsilon h_i M(t).$$

□

Proof of (iv): Threshold crossing condition. Let $\Gamma^* = (\Gamma_1^*, \Gamma_2^*)$ be as in (A5), and suppose there exists a finite time t_c such that

$$M(t_c) \geq \max_{i=1,2} \frac{(\Gamma_i^* - \Gamma_i(0))_+}{\varepsilon h_i}.$$

By part (iii),

$$\Gamma_i(t_c) \geq \Gamma_i(0) + \varepsilon h_i M(t_c).$$

Therefore, for each $i = 1, 2$,

$$\Gamma_i(t_c) \geq \Gamma_i(0) + (\Gamma_i^* - \Gamma_i(0))_+ \geq \Gamma_i^*.$$

Since K_{tot} is non-decreasing in each argument,

$$K_{\text{tot}}(\Gamma(t_c)) \geq K_{\text{tot}}(\Gamma^*).$$

By (A5),

$$|\Delta\omega| < K_{\text{tot}}(\Gamma^*) \sin \bar{\phi},$$

and therefore

$$|\Delta\omega| < K_{\text{tot}}(\Gamma(t_c)) \sin \bar{\phi}.$$

Thus, sufficient accumulated compatibility-window exposure implies crossing of the compatibility-window threshold.

The same conclusion also holds under the componentwise condition

$$\Gamma_i(t_c) \geq \Gamma_i^*, \qquad i = 1, 2,$$

by the same monotonicity argument. □

Proof of (v): Forward invariance. If the threshold condition holds at time t_c, then

$$|\Delta\omega| < K_{\text{tot}}(t_c) \sin \bar{\phi}.$$

Since the threshold inequality is strict at t_c, define

$$\eta_c := K_{\text{tot}}(t_c) \sin \bar{\phi} - |\Delta\omega| > 0.$$

By monotonicity of K_{tot}, the same margin persists for all $t \geq t_c$ with $t \in I_{\max}$:

$$K_{\text{tot}}(t) \sin \bar{\phi} - |\Delta\omega| \geq \eta_c.$$

Let

$$\overline{U}_{\bar{\phi}} := [-\bar{\phi}, \bar{\phi}], \qquad U_{\bar{\phi}} := (-\bar{\phi}, \bar{\phi}).$$

At the upper boundary $\phi = \bar{\phi}$,

$$\dot{\phi} = \Delta\omega - K_{\text{tot}}(t) \sin \bar{\phi} \leq |\Delta\omega| - K_{\text{tot}}(t) \sin \bar{\phi} \leq -\eta_c < 0.$$

At the lower boundary $\phi = -\bar{\phi}$,

$$\dot{\phi} = \Delta\omega + K_{\text{tot}}(t) \sin \bar{\phi} \geq -|\Delta\omega| + K_{\text{tot}}(t) \sin \bar{\phi} \geq \eta_c > 0.$$

Thus, for all $t \geq t_c$ with $t \in I_{\max}$, the vector field points strictly inward at both boundary points of $\overline{U}_{\bar{\phi}}$. If a trajectory starting in $\overline{U}_{\bar{\phi}}$ were to exit the interval within $I_{\max}$, there would be a first exit time at one of the boundary points. The inward-pointing inequalities at both boundary points contradict the outward derivative required at such a first exit time. Hence, by the standard scalar barrier argument, the closed interval $\overline{U}_{\bar{\phi}}$ is positively invariant for the non-autonomous system.

Because the inward inequalities are strict, a trajectory starting in the open interval $U_{\bar{\phi}}$ cannot reach either boundary in forward time within $I_{\max}$. Hence the open window is positively invariant for post-threshold trajectories that enter it. Therefore,

$$\phi(t_0) \in U_{\bar{\phi}}, \quad t_0 \geq t_c \quad \Longrightarrow \quad \phi(t) \in U_{\bar{\phi}} \quad \text{for all } t \geq t_0, \quad t \in I_{\max}.$$

□

Proof of (vi): Capture upon entry. Assume that the threshold condition holds at time t_c, and suppose there exists a time $t_* \geq t_c$ such that

$$\phi(t_*) \in U_{\bar{\phi}}.$$

By the forward invariance established in part (v), it follows that

$$\phi(t) \in U_{\bar{\phi}} \qquad \text{for all } t \geq t_*, \quad t \in I_{\max}.$$

Thus, once the trajectory enters the compatibility window after threshold crossing, it remains captured there for all later times in $I_{\max}$. □

Proof of (vii): Locking and tracking. Inside $U_{\bar{\phi}}$, the moving frozen equilibrium branch satisfies

$$\Delta\omega = K_{\text{tot}}(t) \sin \phi^*(t).$$

After capture, we use the real representative of $\phi(t)$ in $U_{\bar{\phi}}$, so that the difference

$$e(t) = \phi(t) - \phi^*(t)$$

is well-defined. Let

$$e(t) = \phi(t) - \phi^*(t), \qquad V(t) = \frac{1}{2} e(t)^2.$$

Then

$$\dot{e} = -K_{\text{tot}}(t)\big(\sin \phi - \sin \phi^*(t)\big) - \dot{\phi}^*(t).$$

By the mean value theorem,

$$\sin \phi - \sin \phi^*(t) = \cos \xi(t)\, e(t),$$

where $\xi(t)$ lies between $\phi(t)$ and $\phi^*(t)$. Since both $\phi(t)$ and $\phi^*(t)$ lie in $U_{\bar{\phi}}$,

$$\cos \xi(t) \geq \cos \bar{\phi} > 0.$$

Thus,

$$\dot{V} \leq -K_{\text{tot}}(t) \cos \bar{\phi}\, e^2 + |e|\, |\dot{\phi}^*(t)|.$$

Fix a finite post-capture interval

$$[t_*, t_* + L] \subset I_{\max},$$

where $L < \infty$ is fixed independently of ε, and suppose that the corresponding family of captured trajectories $\Gamma(t)$ remains in an ε-independent compact subset of $\mathbb{R}^2_+$ on this interval.

Since F is bounded and H_i is locally bounded, there exists a constant $C > 0$, independent of ε, such that

$$|H_i(F(\phi(t)), \Gamma_i(t))| \leq C, \qquad t \in [t_*, t_* + L] \subset I_{\max}.$$

Therefore,

$$|\dot{\Gamma}_i(t)| = \varepsilon |H_i(F(\phi(t)), \Gamma_i(t))| \leq C\varepsilon,$$

so

$$\dot{\Gamma}_i(t) = O(\varepsilon)$$

on $[t_*, t_* + L] \subset I_{\max}$, with constants independent of ε.

By (A6), K_{tot} is C^1 on a neighborhood of this compact set, with partial derivatives bounded on the compact set. Therefore,

$$\dot{K}_{\text{tot}}(t) = \sum_i \frac{\partial K_{\text{tot}}}{\partial \Gamma_i}(\Gamma(t))\dot{\Gamma}_i(t) = O(\varepsilon)$$

on $[t_*, t_* + L] \subset I_{\max}$.

Since $\Gamma(t)$ is C^1, it follows that $K_{\mathrm{tot}}(t) = K_{\mathrm{tot}}(\Gamma(t))$ is C^1 on the post-capture interval. Moreover, because the moving frozen equilibrium branch satisfies

$$\phi^*(t) = \arcsin\left(\frac{\Delta\omega}{K_{\mathrm{tot}}(t)}\right),$$

with arcsin taken on the principal branch, $\phi^*(t)$ is C^1 on the interval as well.

Differentiating the equilibrium-branch condition

$$\Delta\omega = K_{\mathrm{tot}}(t)\sin\phi^*(t)$$

gives

$$0 = \dot{K}_{\mathrm{tot}}(t)\sin\phi^*(t) + K_{\mathrm{tot}}(t)\cos\phi^*(t)\dot{\phi}^*(t).$$

Hence,

$$\dot{\phi}^*(t) = -\frac{\dot{K}_{\mathrm{tot}}(t)}{K_{\mathrm{tot}}(t)}\tan\phi^*(t).$$

Since $\phi^*(t) \in U_{\bar{\phi}}$, we have

$$|\tan\phi^*(t)| \le C_0.$$

Moreover, the compatibility-window threshold gives

$$K_{\mathrm{tot}}(t) > \frac{|\Delta\omega|}{\sin\bar{\phi}} \qquad \text{for all } t \ge t_c,$$

so $K_{\mathrm{tot}}(t)$ is bounded away from zero uniformly on the post-threshold interval. Since $\dot{K}_{\mathrm{tot}}(t) = O(\varepsilon)$, we obtain

$$|\dot{\phi}^*(t)| \le C\varepsilon$$

on $[t_*, t_* + L] \subset I_{\max}$.

Since the compatibility-window threshold persists for $t \ge t_c$, define

$$\lambda_0 := |\Delta\omega|\cot\bar{\phi} > 0.$$

Then

$$K_{\mathrm{tot}}(t)\cos\bar{\phi} \ge \lambda_0 \qquad \text{for all } t \ge t_c, \quad t \in I_{\max}.$$

Therefore,

$$\dot{V} \le -2\lambda_0 V + |e|\,|\dot{\phi}^*(t)|.$$

Using Young's inequality,

$$|e|\,|\dot{\phi}^*(t)| \le \frac{\lambda_0}{2}e^2 + \frac{1}{2\lambda_0}|\dot{\phi}^*(t)|^2.$$

Therefore,

$$\dot{V} \le -2\lambda_0 V + \frac{\lambda_0}{2}e^2 + \frac{1}{2\lambda_0}|\dot{\phi}^*(t)|^2.$$

Since $e^2 = 2V$ and $|\dot{\phi}^*(t)| \le C\varepsilon$, this yields

$$\dot{V} \le -\lambda_0 V + C\varepsilon^2.$$

By Grönwall's inequality,

$$V(t) \le e^{-\lambda_0(t-t_*)}V(t_*) + C_L\varepsilon^2, \qquad t \in [t_*, t_* + L] \subset I_{\max}.$$

Therefore,

$$|e(t)| \le e^{-\lambda_0(t-t_*)/2}|e(t_*)| + C_L\varepsilon, \qquad t \in [t_*, t_* + L] \subset I_{\max}.$$

Equivalently,

$$|\phi(t) - \phi^*(t)| \le e^{-\lambda_0(t-t_*)/2}|\phi(t_*) - \phi^*(t_*)| + C_L\varepsilon, \qquad t \in [t_*, t_* + L] \subset I_{\max}.$$

If

$$|\phi(t_*) - \phi^*(t_*)| = O(\varepsilon),$$

then

$$\phi(t) = \phi^*(t) + O(\varepsilon)$$

on $[t_*, t_* + L] \subset I_{\max}$.

More generally, the captured trajectory satisfies a stability estimate consisting of an exponentially decaying entry-error term plus an $O(\varepsilon)$ forcing term on finite post-capture intervals of length L fixed independently of ε. Full $O(\varepsilon)$ tracking follows whenever the entry error is $O(\varepsilon)$.

Finally,

$$\sin \phi^*(t) = \frac{\Delta\omega}{K_{\text{tot}}(t)},$$

so

$$\phi^*(t) \to 0 \qquad \text{as } K_{\text{tot}}(t) \to \infty.$$

This proves part (vii). □

Conclusion. All statements of Theorem 1 are established.

6. Dynamical phenomena and interpretation

6.1. Conditional drift-to-capture transition

We describe the conditional transition from drift to capture and finite-interval tracking induced by accumulation-mediated coupling.

Subthreshold regime. If

$$K_{\text{tot}}(t) < |\Delta\omega|,$$

the system is in the drift regime. The lifted phase evolves monotonically, and on compact uniformly subthreshold intervals the projected phase performs rotations on $\mathbb{S}^1$. In the corresponding frozen dynamics, no phase-locked equilibria exist. During this regime, each completed rotation produces compatibility-window exposure through traversal of $U_{\bar{\phi}}$.

Accumulation and threshold crossing. During drift, traversal of the compatibility window produces residence-time exposure measured by $M(t)$. This exposure gives a guaranteed positive contribution to the growth of the integration variables $\Gamma_i(t)$, and hence may increase $K_{\text{tot}}(t)$ through the monotone coupling map.

If compatibility-window exposure reaches the sufficient level specified in Theorem 1(iv) by a finite time t_c, then

$$K_{\text{tot}}(t_c) \sin \bar{\phi} > |\Delta\omega|.$$

This condition corresponds to the compatibility-window threshold, which is stronger than the equilibrium-existence condition

$$K_{\text{tot}}(t) > |\Delta\omega|.$$

Capture. For $t \geq t_c$, with $t \in I_{\max}$,

$$K_{\text{tot}}(t) \sin \bar{\phi} > |\Delta\omega|,$$

so the compatibility window becomes forward-invariant in the sense established in Section 5.5.

If the trajectory enters $U_{\bar{\phi}}$ at some time $t_* \geq t_c$, then Section 5.5 implies capture:

$$\phi(t) \in U_{\bar{\phi}} \qquad \text{for all } t \geq t_*, \quad t \in I_{\max}.$$

Thus, confinement is not imposed a priori. It occurs conditionally, after compatibility-window threshold crossing and post-threshold entry.

Locking and tracking. Inside $U_{\bar{\phi}}$, the captured trajectory is compared with the moving frozen equilibrium branch $\phi^*(t)$. Section 5.6 establishes finite-interval tracking on shifted post-capture intervals. Specifically, the deviation satisfies a stability estimate consisting of an exponentially decaying entry-error term plus an $O(\varepsilon)$ forcing term.

Full $O(\varepsilon)$ tracking on the finite interval follows whenever the entry error is already $O(\varepsilon)$.

Summary.

$$\begin{aligned}&\text{drift/traversal} \Longrightarrow \text{exposure-driven accumulation}\\&\Longrightarrow \text{threshold crossing when sufficient exposure is attained}\\&\Longrightarrow \text{capture upon post-threshold entry} \Longrightarrow \text{finite-interval tracking.}\end{aligned}$$

6.2. Accumulation delay and synchronization-like capture

Along trajectories where sufficient exposure produces threshold crossing and post-threshold entry occurs, synchronization-like capture occurs after an accumulation delay.

Initial regime. If

$$K_{\text{tot}}(0) < |\Delta\omega|,$$

the system begins in the drift regime, and no phase-locked states exist under the frozen dynamics. In this phase, the coupling is insufficient to overcome detuning, and the phase difference evolves without sustained alignment.

Finite delay. The integration variables evolve with rate $O(\varepsilon)$, corresponding to a slow timescale of order $O(1/\varepsilon)$, and their growth receives a guaranteed positive contribution from compatibility-window exposure. This accumulation introduces a trajectory-dependent delay between initial conditions and possible compatibility-window threshold crossing.

If sufficient accumulated exposure is attained, there exists a finite threshold-crossing time $t_c > 0$ such that

$$K_{\text{tot}}(t_c)\sin\bar{\phi} > |\Delta\omega|.$$

If t_c denotes the first time at which the compatibility-window threshold is crossed, then for $t < t_c$ the compatibility window has not yet become forward-invariant. For $t \geq t_c$, with $t \in I_{\max}$, the compatibility window is forward-invariant; capture occurs only upon post-threshold entry into the window.

Parameter dependence. The delay depends on system parameters:

- smaller ε tends to increase the accumulation timescale;
- larger $|\Delta\omega|$ increases the compatibility-window threshold that must be reached;
- larger initial $\Gamma_i(0)$ can reduce the additional accumulation needed to reach the threshold.

These parameters influence the accumulation timescale in the model, but the actual threshold-crossing delay remains trajectory-dependent.

Consequence. Phase locking/capture emerges after a finite accumulation period only for trajectories satisfying the exposure and entry conditions. Thus, synchronization-like capture is not determined by initial coupling alone, but by the trajectory-level accumulation and post-threshold entry mechanism established in Section 5.

6.3. Memory and accumulation effects

The integration variables introduce trajectory-dependent memory into the coupling dynamics.

Accumulation. The evolution

$$\dot{\Gamma}_i = \varepsilon H_i(F(\phi), \Gamma_i)$$

implies that $\Gamma_i(t)$ aggregates contributions over time.

By the compatibility-window growth assumption, residence time inside $U_{\bar{\phi}}$ provides a guaranteed positive contribution to integration growth. Growth outside the compatibility window is not excluded by the assumptions. Thus, transient visits to the compatibility window can leave persistent imprints on the integration state.

History dependence. The effective coupling $K_{\mathrm{tot}}(t)$ depends on the accumulated variables $\Gamma_i(t)$, and therefore on the past trajectory rather than only on the instantaneous phase value. As a result, identical phase configurations may correspond to different effective couplings depending on prior evolution.

Irreversibility. Under (A1),

$$\Gamma_i(t_2) \geq \Gamma_i(t_1), \qquad t_2 \geq t_1.$$

This monotonicity implies that accumulated integration cannot be undone by subsequent dynamics.

Consequence. Repeated transient visits to the compatibility window can produce cumulative growth of $\Gamma_i(t)$, yielding monotone amplification of $K_{\mathrm{tot}}(t)$ and possible threshold crossing when sufficient compatibility-window exposure is accumulated.

The resulting mechanism is therefore history-dependent. Under genuine hidden-state dependence, it cannot be represented for all admissible histories by universal phase-only update laws of the form

$$\dot{K} = f(\phi).$$

6.4. Intermittent and partial synchronization

We describe possible intermediate behavior near the compatibility-window threshold. These regimes are qualitative interpretations of the dynamics and are not asserted as universal outcomes.

Near-threshold dynamics. If

$$K_{\mathrm{tot}}(t) \sin \bar{\phi} \approx |\Delta\omega|,$$

the phase velocity may become small near points satisfying

$$\sin \phi \approx \frac{\Delta\omega}{K_{\mathrm{tot}}(t)}.$$

This slowing reflects the near-balance between detuning and coupling in the frozen dynamics.

Intermittent confinement. Before the compatibility window becomes forward-invariant, trajectories may enter and exit low-incompatibility regions. In this regime, intervals of reduced phase velocity near frozen near-equilibrium points may alternate with faster drift across the remainder of $\mathbb{S}^1$.

This behavior is consistent with the absence of a trapping region before the compatibility-window threshold is satisfied.

Partial synchronization. In such near-threshold regimes, $\phi(t)$ may spend an increased fraction of time in regions of low incompatibility, yielding reduced average incompatibility without strict phase locking. The dynamics may therefore exhibit a bias toward alignment while remaining globally drifting.

Transition. If $K_{\mathrm{tot}}(t)$ increases sufficiently along a trajectory so that the compatibility-window threshold is reached,

$$K_{\mathrm{tot}}(t) \sin \bar{\phi} > |\Delta\omega|,$$

then the compatibility window becomes forward-invariant as described in Section 5.5. Any trajectory that enters the window after threshold crossing is captured, and the finite-interval tracking estimate of Section 5.6 applies from the entry time onward.

7. Numerical illustration of the conditional accumulation-driven mechanism

7.1. Model specification

We consider a system satisfying Assumptions (A1)–(A6), and write

$$K_{\mathrm{tot}}(t) := K_{\mathrm{tot}}(\Gamma_1(t), \Gamma_2(t)).$$

The simulations below illustrate one admissible trajectory for which compatibility-window exposure accumulates sufficiently to produce threshold crossing, followed by post-threshold entry and finite-interval tracking. They are not used to prove unconditional threshold crossing or unconditional capture for all admissible trajectories.

Dynamical system. The simulated system is

$$\dot{\phi} = \Delta\omega - K_{\mathrm{tot}}(t)\sin\phi, \qquad \dot{\Gamma}_i = \varepsilon H_i(F(\phi), \Gamma_i), \qquad i = 1, 2,$$

with

$$F(\phi) = 1 - \cos\phi.$$

Integration dynamics. We take

$$H_i(F, \Gamma_i) = \frac{a_i}{1+F}, \qquad a_i > 0.$$

This choice is non-negative for all $F \geq 0$, and is larger when F is smaller. For this choice, integration growth is larger when incompatibility is smaller.

On the compatibility window

$$U_{\bar{\phi}} = (-\bar{\phi}, \bar{\phi}),$$

we have

$$F(\phi) \leq 1 - \cos\bar{\phi}.$$

Therefore,

$$H_i(F(\phi), \Gamma_i) \geq \frac{a_i}{1 + 1 - \cos\bar{\phi}} > 0,$$

so Assumptions (A1)–(A2) are satisfied.

Effective coupling. The effective coupling is

$$K_{\mathrm{tot}}(t) = \kappa(1 + \Gamma_1(t))(1 + \Gamma_2(t)), \qquad \kappa > 0.$$

This form is continuous, non-decreasing in each Γ_i, and unbounded as the integration variables grow. Thus it satisfies Assumption (A3), and the threshold reachability condition (A5) is satisfied for sufficiently large (Γ_1, Γ_2).

Parameters and compatibility window. The parameters are

$$\Delta\omega = 1, \qquad \varepsilon = 0.05, \qquad a_1 = a_2 = 1, \qquad \kappa = 0.2,$$

with compatibility window

$$U_{\bar{\phi}} = (-\bar{\phi}, \bar{\phi}), \qquad \bar{\phi} = 0.6.$$

The corresponding thresholds are

$$|\Delta\omega| = 1,$$

and

$$\frac{|\Delta\omega|}{\sin\bar{\phi}} = \frac{1}{\sin(0.6)}.$$

The second threshold is the compatibility-window threshold associated with forward invariance; capture occurs upon post-threshold entry into the window.

Initial conditions. The initial conditions are

$$\phi(0) = 2.0, \qquad \Gamma_1(0) = \Gamma_2(0) = 0.$$

Thus

$$K_{\mathrm{tot}}(0) = 0.2 < |\Delta\omega|,$$

so the system starts in the drift regime.

Numerical scheme. The system is integrated using a fourth-order Runge–Kutta method with fixed time step

$$\Delta t = 10^{-3}.$$

The time horizon is chosen sufficiently large to display the full observed sequence in this parameter set: drift/traversal, accumulation, threshold crossing, post-threshold entry, capture, and finite-interval tracking.

7.2. Drift and compatibility traversal

We examine the phase dynamics in the initial subthreshold regime.

Drift regime. With the parameters of Section 7.1,

$$K_{\text{tot}}(0) < |\Delta\omega|,$$

so the simulated trajectory begins in the drift regime. In this regime, $\dot{\phi}(t)$ does not vanish, the lifted phase evolves monotonically, and the projected phase rotates on $\mathbb{S}^1$. This behavior is consistent with the drift regime characterized in Section 5.3.

Phase evolution. Numerical integration shows continuous rotations of $\phi(t)$ at early times, with no approach to a frozen equilibrium branch. This illustrates the absence of phase locking in the simulated early-time subthreshold regime.

Figure 1 shows the wrapped phase during the initial drift regime and the observed near-threshold slowing.

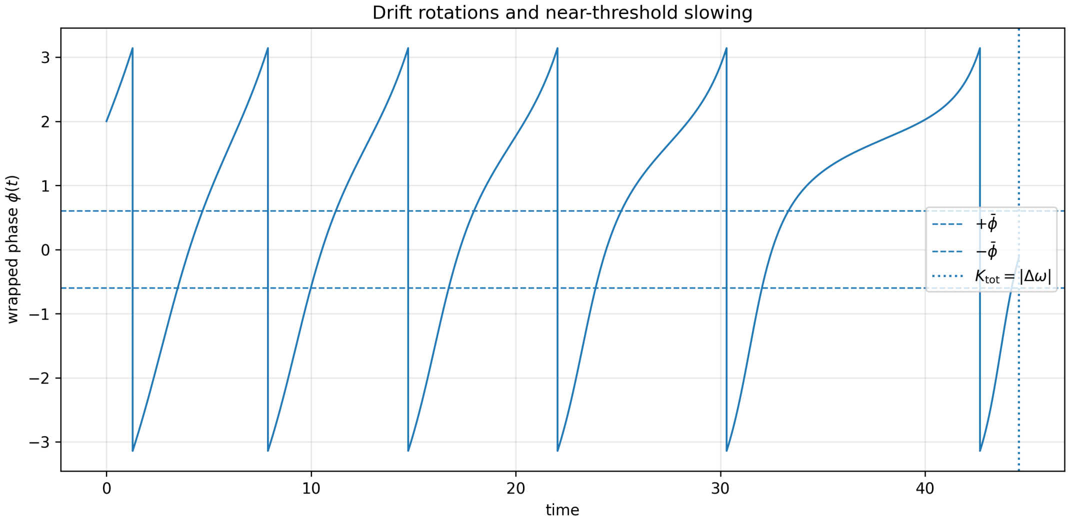

Figure 1: Drift rotations and near-threshold slowing in the simulated trajectory. The wrapped phase performs repeated rotations on $\mathbb{S}^1$ while the effective coupling remains below the ordinary equilibrium threshold. As $K_{\text{tot}}(t)$ approaches $|\Delta\omega|$, the phase velocity slows, illustrating the transition from drift toward near-threshold dynamics.

Compatibility traversal. In the simulated trajectory, the phase repeatedly traverses the compatibility window

$$U_{\bar{\phi}} = (-\bar{\phi}, \bar{\phi}).$$

During each rotation, the phase passes through this interval, producing repeated visits to low-incompatibility configurations. This behavior is consistent with the traversal mechanism analyzed in Section 5.3 on compact uniformly subthreshold intervals.

Figure 2 shows the repeated traversal of the compatibility window before post-threshold capture.

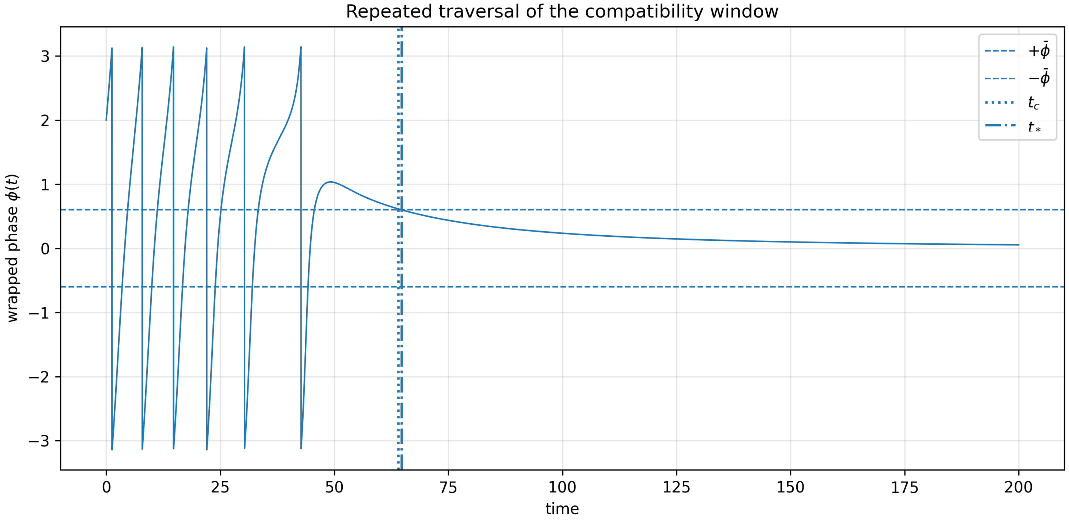

Figure 2: Repeated traversal of the compatibility window in the simulated trajectory. Before post-threshold capture, the wrapped phase repeatedly crosses $U_{\bar{\phi}}$, producing compatibility-window residence-time exposure. The marked times t_c and t_* denote the simulated compatibility-window threshold crossing and post-threshold entry times.

Consequence. In the simulated trajectory, drift rotations generate repeated compatibility-window residence-time contributions, providing the exposure input used in the accumulation estimate of Section 5.4.

7.3. Integration growth and threshold crossing

We examine the growth of the integration variables and the resulting amplification of the effective coupling in the simulated trajectory.

Integration growth. The integration dynamics are

$$\dot{\Gamma}_i = \varepsilon H_i(F(\phi), \Gamma_i), \qquad H_i(F, \Gamma_i) = \frac{a_i}{1 + F(\phi)}.$$

Numerical results show that $\Gamma_i(t)$ increase monotonically. The scaled cumulative window time $\varepsilon M(t)$ provides a reference for the guaranteed contribution from compatibility-window exposure described in Section 5.4. Growth outside the compatibility window is not excluded by the model.

Figure 3 shows the monotone growth of the integration variables together with the compatibility-window exposure reference.

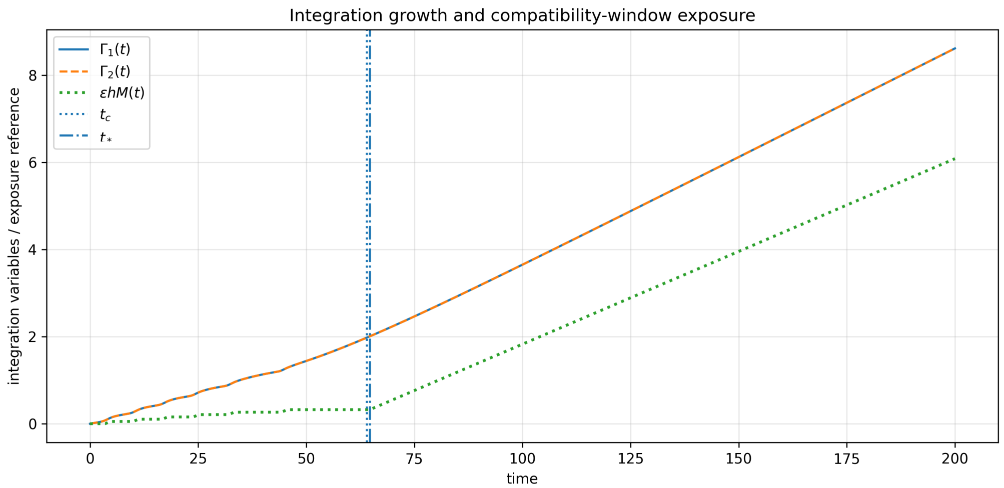

Figure 3: Growth of integration variables in the simulated trajectory. The variables $\Gamma_i(t)$ increase monotonically. The scaled lower-bound reference $\varepsilon h M(t)$ represents the guaranteed contribution from compatibility-window exposure; additional growth outside the window is not excluded by the model.

Coupling amplification. The effective coupling

$$K_{\rm tot}(t) = \kappa(1+\Gamma_1(t))(1+\Gamma_2(t))$$

increases monotonically with $\Gamma_i(t)$, consistent with Assumption (A3). In the simulated trajectory, this monotone amplification reflects the accumulated growth of the integration variables.

Threshold crossing. Two thresholds are relevant:

$$\text{equilibrium threshold:} \qquad K_{\rm tot}(t) = |\Delta\omega|,$$

and

$$\text{compatibility-window threshold:} \qquad K_{\rm tot}(t)\sin\bar{\phi} = |\Delta\omega|.$$

In the simulated trajectory, compatibility-window exposure accumulates sufficiently for the effective coupling to cross the compatibility-window threshold at a finite time t_c:

$$K_{\rm tot}(t_c)\sin\bar{\phi} > |\Delta\omega|.$$

This is consistent with the exposure-based threshold-crossing condition of Theorem 1(iv).

Figure 4 shows the ordinary equilibrium threshold and the stronger compatibility-window threshold in the simulated trajectory.

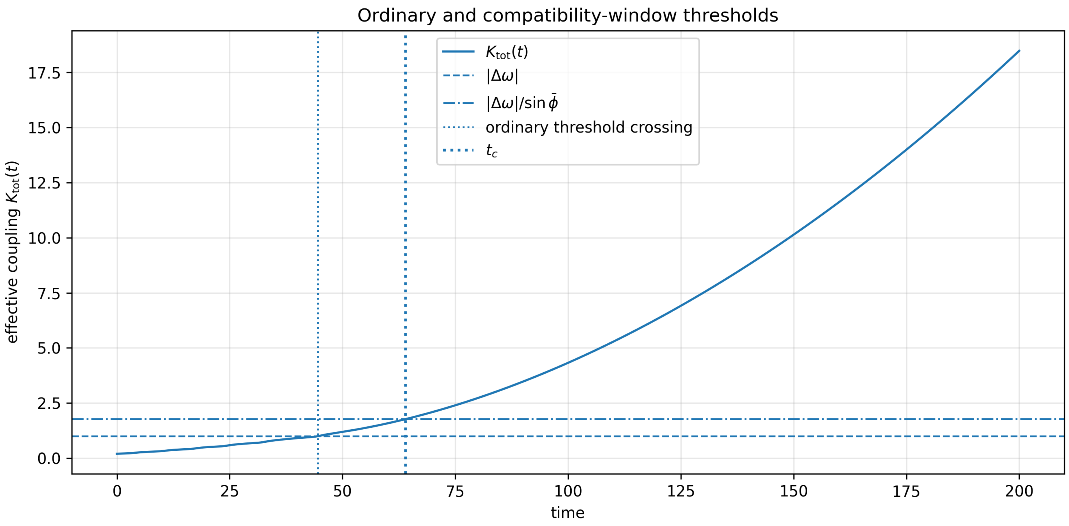

Figure 4: Threshold structure in the simulated trajectory. The effective coupling crosses the ordinary equilibrium threshold $K_{\rm tot} = |\Delta\omega|$ before crossing the compatibility-window threshold $K_{\rm tot} = |\Delta\omega|/\sin\bar{\phi}$. The marked time t_c denotes the observed crossing of the compatibility-window threshold for this trajectory.

Consequence. For this simulated trajectory, the effective coupling reaches the compatibility-window threshold in finite time. After this crossing, the compatibility window is forward-invariant; capture still depends on post-threshold entry into the window.

7.4. Capture and finite-interval tracking

We examine the dynamics after compatibility-window threshold crossing in the simulated trajectory.

Post-threshold regime. For $t \geq t_c$, within the simulated interval,

$$|\Delta\omega| < K_{\mathrm{tot}}(t) \sin \bar{\phi},$$

so the compatibility window $U_{\bar{\phi}}$ is forward-invariant, in agreement with Section 5.5.

Entry. In this simulated trajectory, after threshold crossing, the trajectory enters $U_{\bar{\phi}}$ at a finite time $t_* \geq t_c$. Section 5.5 then implies that the trajectory remains captured in the compatibility window for later times within the simulated interval.

Capture. For $t \geq t_*$ within the simulated interval,

$$\phi(t) \in U_{\bar{\phi}},$$

and the trajectory remains confined within the compatibility window.

Figure 5 shows post-threshold entry, capture inside the compatibility window, and the post-capture tracking error.

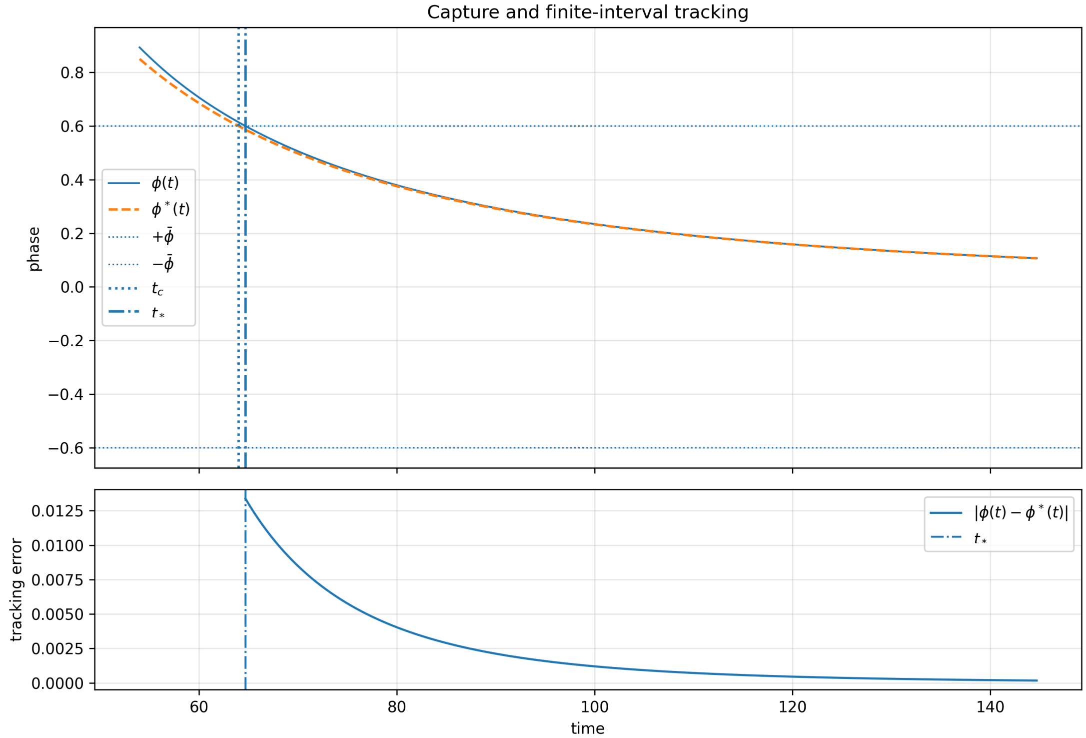

Figure 5: Capture and finite-interval tracking of the moving frozen branch. (a) After the observed compatibility-window threshold-crossing time t_c, the trajectory enters the compatibility window at t_* and remains inside. The captured phase $\phi(t)$ is shown together with the moving frozen equilibrium branch $\phi^*(t)$ and the compatibility-window boundaries. (b) The post-capture tracking error $|\phi(t) - \phi^*(t)|$ decreases over the displayed finite interval, consistent with the finite-interval tracking estimate of Section 5.6.

Locking and tracking. Within $U_{\bar{\phi}}$, the trajectory is compared with the moving frozen equilibrium branch $\phi^*(t)$. The numerical behavior is consistent with the finite-interval tracking estimate of Section 5.6: an exponentially decaying entry-error term plus an $O(\varepsilon)$ forcing term, with full $O(\varepsilon)$ tracking only when the entry error is $O(\varepsilon)$.

Consequence. The simulated trajectory exhibits the conditional sequence predicted by Section 5: threshold crossing, post-threshold entry, capture, and finite-interval tracking of the moving frozen equilibrium branch.

7.5. Finite-interval tracking of the moving frozen branch

We examine the dynamics after capture by comparing the simulated trajectory with the moving frozen equilibrium branch.

Moving frozen branch. For $t \geq t_*$ within the simulated interval,

$$\Delta\omega = K_{\text{tot}}(t)\sin\phi^*(t)$$

defines the moving frozen equilibrium branch $\phi^*(t) \in U_{\bar{\phi}}$, in agreement with the post-capture formulation of Section 5.6.

Tracking. Numerical results show that $\phi(t)$ approaches $\phi^*(t)$ rapidly after capture and remains close over the observed post-capture interval. This behavior is consistent with the finite-interval estimate of Section 5.6:

$$|\phi(t) - \phi^*(t)| \leq e^{-\lambda_0(t-t_*)/2}|\phi(t_*) - \phi^*(t_*)| + C_L\varepsilon.$$

Full $O(\varepsilon)$ tracking on the interval follows when the entry error is $O(\varepsilon)$.

Convergence. Since $K_{\text{tot}}(t)$ increases in the simulation, the moving frozen branch satisfies

$$\phi^*(t) \to 0.$$

The captured trajectory follows this branch according to the finite-interval tracking estimate.

Structure. The simulated dynamics exhibit a fast–slow structure: the phase approaches the moving frozen branch after capture, while the branch itself evolves slowly through the accumulated growth of $K_{\text{tot}}(t)$.

7.6. Parameter dependence in tested trajectories

We examine the dependence of the simulated dynamics on system parameters within the conditional mechanism described above.

Timescale parameter. Smaller ε tends to delay threshold crossing and, when post-threshold entry occurs, capture in the simulated trajectories, while larger ε accelerates the accumulation of the integration variables.

This reflects the role of ε in controlling the rate of accumulation. Across the tested parameter range, the qualitative sequence is preserved for trajectories that accumulate sufficient exposure and enter the window after threshold crossing.

Detuning. Larger $|\Delta\omega|$ delays accumulation and threshold crossing in the tested trajectories, while smaller $|\Delta\omega|$ accelerates them. This dependence arises from the increased compatibility-window threshold required to overcome larger detuning.

Assumption (A5) supplies coupling-level reachability; finite-time crossing is observed in the tested trajectories when sufficient compatibility-window exposure accumulates.

Initial conditions. Larger initial $\Gamma_i(0)$ lead to earlier threshold crossing in the tested trajectories. Smaller initial values prolong the drift phase and delay threshold crossing in the tested trajectories; capture still depends on sufficient exposure and post-threshold entry.

Consequence. Parameter variations affect the timing of the observed transition but preserve the conditional qualitative sequence

$$\begin{aligned}&\text{drift/traversal} \Longrightarrow \text{exposure-driven accumulation}\\ &\Longrightarrow \text{threshold crossing when sufficient exposure is attained}\\ &\Longrightarrow \text{capture upon post-threshold entry} \Longrightarrow \text{finite-interval tracking.}\end{aligned}$$

Within the tested parameter choices, the simulations exhibit the same conditional qualitative sequence for trajectories that accumulate sufficient exposure and enter the window after threshold crossing.

8. Discussion

8.1. Fixed-coupling Kuramoto/Adler setting

We position the present framework relative to classical and adaptive Kuramoto-type models.

Classical Kuramoto setting. In the standard Kuramoto model, coupling is fixed. Synchronization occurs only when the coupling exceeds a critical threshold relative to detuning; otherwise, the system remains in a persistent drift regime. The outcome is determined entirely by instantaneous parameters [2, 9, 12, 1, 11].

Adaptive coupling models. Adaptive and co-evolving phase-oscillator formulations introduce time-dependent coupling, often through phase-dependent or state-dependent update rules, typically represented in simplified form as

$$\dot{K} = f(\phi),$$

so that coupling evolves directly as a function of the instantaneous phase difference. Such formulations are Markovian on the phase–coupling variables and do not, without additional hidden state variables, encode the separate compatibility-exposure history used in the present model. They can produce complex collective behavior, but the evolution of coupling is determined by the current configuration unless additional state variables are introduced [3, 4, 8, 6].

Structural distinction. The present framework differs at the level of coupling generation. Instead of direct dependence on the phase difference, it introduces a compatibility–integration cascade:

$$\phi \longrightarrow F(\phi) \longrightarrow \Gamma_i \longrightarrow K_{\text{tot}}.$$

In this structure:

- coupling is not a function of the instantaneous phase difference;
- it is generated through accumulated contributions over time;
- its evolution depends on the history of compatibility exposure.

Dynamical consequences. This structural difference produces a distinct synchronization-like capture mechanism:

- synchronization-like capture can arise from an initially subthreshold regime when sufficient compatibility-window exposure is accumulated and post-threshold entry occurs;
- the transition occurs conditionally after sufficient accumulated exposure produces compatibility-window threshold crossing;
- drift dynamics generate compatibility-window exposure through repeated traversal, which may drive threshold crossing when sufficient exposure is accumulated.

In contrast, under genuine hidden-state dependence, universal phase-only adaptive laws of the form

$$\dot{K} = f(\phi)$$

cannot reproduce the full augmented trajectory family of the present model without additional state variables.

Interpretation. The compatibility–integration cascade separates instantaneous phase interaction from slow integration dynamics. As a result, synchronization-like capture is not triggered by instantaneous alignment alone, but may emerge when accumulated compatibility exposure drives the system past the compatibility-window threshold and the trajectory subsequently enters the window.

Conclusion. The mechanism established in Section 5 is distinct from classical fixed-coupling Kuramoto dynamics and, under genuine hidden-state dependence, is not reducible to universal phase-only adaptive laws of the form

$$\dot{K} = f(\phi).$$

It arises from a history-dependent coupling structure in which drift, compatibility, and integration jointly produce conditional accumulation-driven capture and finite-interval tracking.

8.2. Structural vs dynamical novelty

We distinguish between the structural elements of the model and the dynamical phenomena they generate in order to clarify the contribution of this work.

Structural framework. The model introduces a compatibility–integration cascade in which effective coupling is generated through an intermediate integration process driven by an incompatibility functional. The defining features are:

- separation between fast phase dynamics and slow integration dynamics;
- a scalar incompatibility functional governing local alignment;
- internal variables that accumulate contributions over time;
- coupling generated as a monotone function of accumulated integration.

Elements of this type appear in various adaptive or co-evolving dynamical systems. The structural components alone are therefore not, in isolation, the primary source of novelty.

Dynamical mechanism. The contribution lies in the dynamical consequences of this structure. The analysis in Section 5 establishes a mechanism with the following properties:

- repeated traversal of the compatibility window produces compatibility-window exposure and corresponding guaranteed accumulation;
- accumulation drives monotone amplification of effective coupling;
- the compatibility-window threshold is crossed when sufficient exposure is accumulated;
- after threshold crossing, a forward-invariant compatibility region forms, and trajectories are trapped upon post-threshold entry;
- the captured phase satisfies finite-interval tracking of the moving frozen equilibrium branch.

This defines a conditional drift-to-capture transition generated internally by the accumulation dynamics.

Nature of novelty. The novelty is therefore dynamical. The key result is that the compatibility–integration structure supports a conditional accumulation-driven transition from drift to capture under the stated monotone accumulation assumptions. In particular, the mechanism yields:

- amplification of coupling from subthreshold initial conditions;
- delayed synchronization-like capture following sufficient compatibility-window exposure;
- capture via forward-invariant regions after threshold crossing and post-threshold entry;
- finite-interval tracking of a moving frozen equilibrium branch.

These properties arise from the interaction between fast phase evolution and slow integration, rather than from instantaneous coupling rules.

Comparison with existing approaches. In standard adaptive models, coupling evolves as a function of instantaneous phase differences or local update rules. While such systems can exhibit complex behavior, they do not, in general, guarantee a transition from drift to locking without imposing additional structure.

In contrast, the present framework identifies exposure and entry conditions under which accumulation-driven synchronization-like capture occurs within the model assumptions.

Interpretation. The model represents a class of systems in which:

- local compatibility is accumulated over time;
- accumulated effects amplify interaction strength;
- conditional drift-to-capture transitions may emerge from repeated local compatibility exposure.

Conclusion. The structural formulation provides the framework, but the contribution is the identification and rigorous derivation of a conditional accumulation-driven synchronization-like capture mechanism that does not rely on instantaneous coupling alone.

8.3. Limitations and extensions

We outline the scope of the present analysis and indicate directions for extension.

Scope of the analysis. The results apply to a two-oscillator system with scalar phase dynamics and a single effective coupling generated through integration variables. The analysis establishes:

- accumulation-driven amplification of coupling;
- exposure-based sufficient conditions for finite-time crossing of the compatibility-window threshold;
- formation of a forward-invariant compatibility region after threshold crossing;
- finite-interval tracking of a moving frozen equilibrium branch after capture.

These results follow from the structural assumptions and conditional hypotheses stated in Section 5.

Limitations. Low-dimensional setting. The analysis is restricted to a pair of oscillators on $\mathbb{S}^1$. Extensions to multi-oscillator systems may introduce additional phenomena, including clustering, frustration, and topology-dependent effects, which can interact with the accumulation mechanism.

Monotone integration dynamics. The integration variables are assumed to be non-decreasing. This ensures persistent accumulation and is a structural condition underlying the results, but excludes:

- decay or forgetting mechanisms;
- saturation effects;
- competitive growth dynamics.

Such effects may modify or bound the accumulation process in extended models.

Local trapping mechanism. The capture result relies on the formation of a forward-invariant compatibility window. This guarantees confinement after entry but does not constitute a fully global characterization of capture in more general dynamical settings.

Timescale separation. The analysis assumes sufficiently small ε, as required in the finite-interval tracking estimates. Behavior outside this regime is not addressed and may lead to qualitatively different dynamics.

Extensions. Higher-dimensional configurations. The compatibility–integration framework could be extended to higher-dimensional manifolds, such as $\mathbb{T}^n$, where incompatibility is defined through geometric misalignment in multiple dimensions.

Networked systems. Generalization to oscillator networks would place the present mechanism in the setting of coupled oscillator and complex network synchronization theory [11, 1, 7, 5]. Such extensions would allow analysis of:

- collective synchronization patterns;
- cluster formation;
- interaction between network topology and accumulation dynamics.

Non-monotone integration. Allowing decay or saturation in Γ_i would introduce:

- finite-memory effects;
- balance between accumulation and loss;
- potentially oscillatory or intermittent regimes.

Quantitative delay characterization. While exposure-based sufficient conditions for finite-time compatibility-threshold crossing are established, precise scaling of the delay time with system parameters remains an open problem.

Conclusion. The present work identifies a controlled two-oscillator setting in which conditional accumulation-driven synchronization-like capture arises rigorously under monotone accumulation, sufficient exposure, and post-threshold entry assumptions. The structural mechanism may persist, with modifications, in more complex and higher-dimensional systems.

9. Conclusion

We have introduced and analyzed a class of phase oscillator systems in which effective coupling is generated through a compatibility–integration cascade. In this framework, interaction strength is not prescribed or directly adapted from instantaneous phase differences, but is generated through integration variables that accumulate compatibility exposure over time.

Main result. Under the structural assumptions (A1)–(A6), we establish that:

- on compact uniformly subthreshold intervals, detuned trajectories repeatedly traverse the compatibility window when the lifted phase completes rotations;
- these traversals produce compatibility-window exposure, which gives a guaranteed positive contribution to the monotone growth of the integration variables;
- the effective coupling increases monotonically, and the compatibility-window threshold is crossed when sufficient exposure is accumulated;
- once the compatibility-window threshold is crossed, the compatibility window becomes forward-invariant; trajectories that enter it after threshold crossing are captured and satisfy finite-interval tracking of the moving frozen equilibrium branch, with full $O(\varepsilon)$ tracking only when the entry error is $O(\varepsilon)$.

Together, these results define a conditional mechanism by which synchronization-like capture may emerge dynamically from an initially subthreshold regime through sufficient compatibility-window exposure and post-threshold entry.

Interpretation. Synchronization-like capture arises here not as an immediate consequence of initial coupling strength, but conditionally through accumulation, amplification, compatibility-window threshold crossing, and post-threshold entry. Transient visits to the compatibility window contribute to persistent changes in the effective coupling, introducing a form of memory that reshapes the dynamics over time.

In this sense, drift is not merely a lack of synchronization, but a regime that can generate compatibility-window exposure, thereby contributing to the conditions required for conditional capture.

Contribution. The primary contribution is the identification and rigorous analysis of a conditional accumulation-driven synchronization-like capture mechanism. While the model is structurally simple, the interaction between fast phase dynamics and slow integration produces the conditional sequence—drift/traversal, exposure-driven accumulation, threshold crossing when sufficient exposure is attained, capture upon post-threshold entry, and finite-interval tracking—that, under genuine hidden-state dependence, cannot be reproduced by universal phase-only adaptive coupling laws of the form

$$\dot{K} = f(\phi).$$

The results isolate structural, exposure, and entry conditions under which synchronization-like capture becomes a conditional outcome of the dynamics rather than an imposed property of the coupling.

Outlook. The compatibility–integration framework provides a basis for studying systems in which interaction strength evolves through accumulated effects. Extensions to higher-dimensional phase spaces, networked oscillators, and non-monotone integration dynamics may extend the mechanism, though the corresponding threshold, capture, and tracking properties would require separate analysis.

Declaration of Generative AI in Scientific Writing

During the preparation of this manuscript, generative AI tools were used to assist with drafting, language editing, and structural development of the text. The author reviewed, edited, and takes full responsibility for the final content of the manuscript.

Data availability

The numerical data and code used to generate the figures are available from the author upon reasonable request.

References

[1] Acebrón, J.A., Bonilla, L.L., Pérez Vicente, C.J., Ritort, F., Spigler, R., 2005. The kuramoto model: A simple paradigm for synchronization phenomena. Reviews of Modern Physics 77, 137–185. doi:10.1103/RevModPhys.77.137.

[2] Adler, R., 1946. A study of locking phenomena in oscillators. Proceedings of the IRE 34, 351–357. doi:10.1109/JRPROC.1946.229930.

[3] Aoki, T., Aoyagi, T., 2009. Co-evolution of phases and connection strengths in a network of phase oscillators. Physical Review Letters 102, 034101. doi:10.1103/PhysRevLett.102.034101.

[4] Aoki, T., Aoyagi, T., 2011. Self-organized network of phase oscillators coupled by activity-dependent interactions. Physical Review E 84, 066109. doi:10.1103/PhysRevE.84.066109.

[5] Arenas, A., Díaz-Guilera, A., Kurths, J., Moreno, Y., Zhou, C., 2008. Synchronization in complex networks. Physics Reports 469, 93–153. doi:10.1016/j.physrep.2008.09.002.

[6] Berner, R., Gross, T., Kuehn, C., Kurths, J., Yanchuk, S., 2023. Adaptive dynamical networks. Physics Reports 1031, 1–59. doi:10.1016/j.physrep.2023.08.001.

[7] Dörfler, F., Bullo, F., 2014. Synchronization in complex networks of phase oscillators: A survey. Automatica 50, 1539–1564. doi:10.1016/j.automatica.2014.04.012.

[8] Gross, T., Blasius, B., 2008. Adaptive coevolutionary networks: A review. Journal of the Royal Society Interface 5, 259–271. doi:10.1098/rsif.2007.1229.

[9] Kuramoto, Y., 1984. Chemical Oscillations, Waves, and Turbulence. Springer, Berlin.

[10] Manzur, O., 2026. Compatibility-modulated stability thresholds in nonlinear dynamical systems: Geometric contraction and network synchronization. URL: https://rebornresearch.com/the-compatibility-integration-cascade/. unpublished manuscript, available on the reBORN Research Initiative website.

[11] Pikovsky, A., Rosenblum, M., Kurths, J., 2001. Synchronization: A Universal Concept in Nonlinear Sciences. Cambridge University Press, Cambridge.

[12] Strogatz, S.H., 2000. From kuramoto to crawford: Exploring the onset of synchronization in populations of coupled oscillators. Physica D: Nonlinear Phenomena 143, 1–20. doi:10.1016/S0167-2789(00)00094-4.